Acta Crystallographica Section B
Structural Science
ISSN 0108-7681

Ferrocene-1,1′-dicarboxylic acid as a building block in supramolecular chemistry: supramolecular structures in one, two and three dimensions

Choudhury M. Zakaria,[a]† George Ferguson,[a,b] Alan J. Lough[c] and Christopher Glidewell[a]*

[a]School of Chemistry, University of St Andrews, St Andrews, Fife KY16 9ST, UK, [b]Department of Chemistry and Biochemistry, University of Guelph, Guelph, Ontario, Canada N1G 2W1, and [c]Lash Miller Chemical Laboratories, University of Toronto, Toronto, Ontario, Canada M5S 3H6

† On leave from Department of Chemistry, University of Rajshahi, Rajshahi, Bangladesh.

Correspondence e-mail: cg@st-andrews.ac.uk

Received 21 May 2002
Accepted 30 May 2002

The supramolecular structures have been determined for nine adducts formed between organic diamines and ferrocene-1,1′-dicarboxylic acid. In the salt-like 1:1 adduct (1) formed with methylamine, the supramolecular structure is one-dimensional, whereas in the 1:1 adducts formed with 1,4-diazabicyclo[2.2.2]octane, (2), and 4,4′-bipyridyl, (4), and in the hydrated 2:1 adduct (3) formed with morpholine, the hard hydrogen bonds form one-dimensional structures, which are expanded to two dimensions by soft C—H···O hydrogen bonds. The hard hydrogen bonds generate two-dimensional structures in the 2:1 adduct (5) formed with octylamine, where the ferrocene component lies across a centre of inversion, in the 1:1 adduct (6) formed with piperidine and in the tetrahydrofuran-solvated 1:1 adduct (7) formed with di(cyclohexyl)amine. In the 2:3 adduct (8) formed by tris-(2-aminoethyl)amine, and in the 2:1 adduct (9) formed with 2-(4′-hydroxyphenyl)ethylamine (tyramine), where $Z' = 1.5$ in space group $P\bar{1}$, the hard hydrogen bonds generate three-dimensional structures. No H transfer from O to N occurs in (4) and only partial transfer of H occurs in (2); in (1), (6) and (7), one H is transferred to N from each acid molecule, and in (3), (5), (8) and (9), two H are transferred from each acid molecule.

1. Introduction

The organometallic diol ferrocene-1,1′-diylbis(diphenylmethanol) $[Fe(C_5H_4CPh_2OH)_2]$ has been found to act as a very versatile building block in supramolecular chemistry and it forms a wide range of supramolecular structures, particularly with organic amines, such that no one structure could be readily predicted even with detailed knowledge of all the others (Ferguson *et al.*, 1993, 1995; Glidewell *et al.*, 1994; Zakaria *et al.*, 2001, 2002*a*,*b*). A characteristic feature of this ferrocenediol is its propensity to form intramolecular O—H···O hydrogen bonds; seeking an analogue from which this characteristic is absent, we have now turned our attention to ferrocene-1,1′-dicarboxylic acid $[Fe(C_5H_4COOH)_2]$, and we present here the synthetic and structural characterization of a range of adducts with organic amines, including primary, secondary and tertiary aliphatic amines, as well as heteroaromatic amines. The materials structurally characterized include: 1:1 adducts formed with dimethylamine [compound (1)], 1,4-diazabicyclo[2.2.2]octane (DABCO) [compound (2)], 4,4′-bipyridyl [compound (4)] and piperidine [compound (6)]; a monohydrated 2:1 adduct with morpholine [compound (3)]; unsolvated 2:1 adducts formed with octylamine [compound (5)] and with 2-(4-hydroxyphenyl)ethylamine [compound (9)]; a 1:1 adduct with di(cyclohexyl)amine, which crystallizes as a tetrahydrofuran hemisolvate [compound (7)]; and a 2:3 adduct formed with tris(2-aminoethyl)amine [compound (8)]. With the primary amines, the dianion $[Fe(C_5H_4COO)_2]^{2-}$ is generally formed, while with secondary amines, formation of the monoanion $[Fe(C_5H_4COO)(C_5H_4COOH)]^-$ is common, although the dianion is present in (3). With the bis-tertiary amine DABCO, there is only partial transfer of H from O to N in (2), while there is no H transfer at all with 4,4′-bipyridyl in (4).

Although the two polymorphic forms of ferrocene-1,1′-dicarboxylic acid were described many years ago (Palenik, 1969; Takusakawa & Koetzle, 1979), little use has been made of this acid and its anions in supramolecular chemistry. Adducts formed between the acid and some bis-amidines have been described (Braga, Maini, Grepioni *et al.*, 2000), but the H atoms of the carboxyl groups in the acid could not be located; nonetheless, both one- and two-dimensional arrays were identified. It is notable that amongst the five structures reported in that study, the two solvent-free systems both generated two-dimensional supramolecular structures, whereas the three solvated systems, incorporating either water or ethanol, gave one-dimensional structures, which is not a readily predictable outcome. Likewise, the 1:1 salts formed with the organometallic cations $[(\eta^5\text{-}C_5H_5)_2Co]^+$ and $[(\eta^5\text{-}C_6H_6)_2Cr]^+$ have been investigated (Braga, Maini & Grepioni, 2000): the dominant behaviour of the ferrocene components was found to be chain formation, with chain-linking either by water molecules or by C—H···O hydrogen-bond formation in which the cations provide the donors.

2. Experimental

2.1. Syntheses

Equimolar quantities of ferrocene-1,1′-dicarboxylic acid and the appropriate amine were separately dissolved, usually in methanol but occasionally in tetrahydrofuran; the solutions were mixed and then set aside to crystallize, yielding compounds (1)–(9). The results of the analyses are:

(1), found C 52.0, H 5.1, N 4.4%; $C_{14}H_{17}FeNO_4$ requires C 52.7, H 5.4, N 4.4%;

(2), found C 56.0, H 5.5, N 6.9%; $C_{18}H_{22}FeN_2O_4$ requires C 56.0, H 5.7, N 7.3%;

(3), found C 52.0, H 6.4, N 5.9%; $C_{20}H_{30}FeN_2O_7$ requires C 52.0, H 6.5, N 6.0%;

(4), found C 61.4, H 3.7, N 6.4%; $C_{22}H_{18}FeN_2O_4$ requires C 61.4, H 4.2, N 6.5%;

(5), found C 63.1, H 9.1, N 5.2%; $C_{28}H_{48}FeN_2O_4$ requires C 63.1, H 9.1, N 35.3%;

(6), found C 56.2, H 5.8, N 3.8%; $C_{17}H_{21}FeNO_4$ requires C 56.8, H 5.9, N 3.9%;

(7), found C 63.5, H 8.2, N 2.8%; $C_{52}H_{74}Fe_2N_2O_9$ requires C 63.5, H 7.6, N 2.9%;

(8), found C 51.2, H 6.4, N 9.4%; $C_{48}H_{66}Fe_3N_8O_{12}$ requires C 51.7, H 6.0, N 10.1%;

(9), found C 60.5, H 6.6, N 4.4%; $C_{28}H_{32}FeN_2O_6$ requires C 61.3, H 5.9, N 5.1%.

Crystals of (1)–(9) suitable for single-crystal X-ray diffraction were selected directly from the analytical samples.

In addition to (1)–(9), a number of other adducts have been synthesized in a similar manner, but for none of these examples have crystals of appropriate quality yet been obtained, although the analytical data are entirely satisfactory. Thus, with the bis-primary aliphatic amine 1,2-diaminoethane, a 1:1 adduct (10) is formed, and the bis-secondary aliphatic amines piperazine and 2,5-dimethylpiperazine give 1:1 adducts (11) and (12), respectively; hexamethylenetetramine, $(CH_2)_6N_4$, gives a 1:1 adduct, (13), analogous to (2); 1,2-bis(4-pyridyl)-ethene gives a 1:1 adduct, (14), analogous to (4); the primary amines *n*-butylamine, *tert*-butylamine, adamantylmethylamine and tris(hydroxymethyl)methylamine all give 2:1 adducts, (15)–(18), respectively, analogous to (5); di(isopropyl)amine forms a 1:1 adduct, (19), analogous to (7); 1:1 adducts (20) and (21), respectively, are also formed by benzylamine and 2,3-diaminopyridine. Analyses for (10)–(21) are:

(10), found C 50.2, H 4.4, N 8.1%; $C_{14}H_{18}FeN_2O_4$ requires C 50.3, H 5.4, N 8.4%;

(11), found C 53.6, H 5.3, N 7.6%; $C_{16}H_{20}FeN_2O_4$ requires C 53.3, H 5.6, N 7.8%;

(12), found C 54.7, H 5.8, N 7.2%; $C_{18}H_{24}FeN_2O_4$ requires C 55.7, H 6.2, N 7.2%;

(13), found C 51.7, H 5.3, N 13.3%; $C_{18}H_{22}FeN_4O_4$ requires C 52.2, H 5.4, N 13.5%;

(14), found C 63.4, H 3.9, N 6.2%; $C_{24}H_{20}FeN_2O_4$ requires C 63.2, H 4.4, N 6.1%;

(15), found C 57.2, H 7.6, N 6.6%; $C_{20}H_{32}FeN_2O_4$ requires C 57.2, H 7.7, N 6.7%;

(16), found C 57.3, H 7.6, N 6.2%; $C_{20}H_{32}FeN_2O_4$ requires C 57.2, H 7.7, N 6.7%;

(17), found C 67.8, H 8.1, N 4.5%; $C_{34}H_{48}FeN_2O_4$ requires C 67.5, H 8.0, N 4.6%;

(18), found C 46.6, H 6.6, N 5.3%; $C_{20}H_{32}FeN_2O_{10}$ requires C 46.5, H 6.3, N 5.4%;

(19), found C 56.1, H 7.1, N 3.7%; $C_{18}H_{25}FeNO_4$ requires C 57.6, H 6.7, N 3.7%;

(20), found C 60.1, H 4.5, N 3.8%; $C_{19}H_{19}FeNO_4$ requires C 59.9, H 5.0, N 3.7%;

(21), found C 52.8, H 3.8, N 10.8%; $C_{17}H_{17}FeN_3O_4$ requires C 53.3, H 4.5, N 11.0%.

2.1.1. Data collection, structure solution and refinement. Diffraction data for (1)–(9) were collected at 150 (2) K using a Nonius KappaCCD diffractometer with graphite-monochromated Mo $K\alpha$ radiation (λ = 0.71073 Å). Other details of cell data, data collection and refinement are summarized in Table 1, together with details of the software employed (Ferguson, 1999; Nonius, 1997; Otwinowski & Minor, 1997; Sheldrick, 1997*a*,*b*; Spek, 2002).

For (1), the systematic absences permitted the space groups *Cc* and *C*2/*c*; *C*2/*c* was selected and subsequently confirmed by successful structure solution and refinement. (2), (4), (5) and (7)–(9) are all triclinic: space group $P\bar{1}$ was selected for each and subsequently confirmed by successful structure solution and refinement. For (3) and (6), the space group $P2_1/c$ was uniquely assigned from the systematic absences. The struc-

Table 1
Experimental details.

	(1)	(2)	(3)	(4)	(5)
Crystal data					
Chemical formula	$(C_2H_8N)[Fe(C_6H_4O_2)\cdot(C_6H_5O_2)]$	$[Fe(C_6H_5O_2)_2]\cdot C_6H_{12}N_2$	$(C_4H_{10}NO)_2[Fe(C_6H_4O_2)_2]\cdot H_2O$	$[Fe(C_6H_5O_2)_2]\cdot C_{10}H_8N_2$	$(C_8H_{20}N)_2[Fe(C_6H_4O_2)_2]$
Chemical formula weight	319.14	386.23	466.31	430.23	532.53
Cell setting, space group	Monoclinic, $C2/c$	Triclinic, $P\bar{1}$	Monoclinic, $P2_1/c$	Triclinic, $P\bar{1}$	Triclinic, $P\bar{1}$
a, b, c (Å)	30.9616 (7), 7.8147 (2), 12.1521 (3)	7.4666 (3), 10.7846 (5), 11.3184 (6)	7.4018 (2), 9.2018 (3), 30.3884 (11)	6.9500 (2), 10.7645 (3), 12.5260 (4)	6.3490 (2), 9.6089 (4), 12.1674 (4)
α, β, γ (°)	90, 109.7090 (12), 90	104.897 (2), 99.153 (2), 105.238 (2)	90, 101.0630 (15), 90	97.8780 (11), 92.0960 (11), 103.0030 (13)	98.738 (2), 100.380 (2), 91.2290 (17)
V (Å^3)	2768.02 (12)	824.32 (7)	2031.29 (11)	902.27 (5)	720.76 (4)
Z	8	2	4	2	1
D_x (Mg m^{-3})	1.532	1.556	1.525	1.584	1.227
Radiation type	Mo $K\alpha$	Mo $K\alpha$	Mo $K\alpha$	Mo $K\alpha$	Mo $K\alpha$
No. of reflections for cell parameters	3330	2733	3487	3636	2871
θ range (°)	2.70–27.50	2.91–25.06	2.60–27.47	3.02–27.50	3.76–27.57
μ (mm^{-1})	1.101	0.941	0.789	0.870	0.557
Temperature (K)	150 (2)	150 (2)	150 (2)	150 (2)	150 (2)
Crystal form, colour	Plate, red	Plate, colourless	Block, red	Needle, colourless	Needle, red
Crystal size (mm)	0.22 × 0.20 × 0.12	0.16 × 0.16 × 0.01	0.18 × 0.14 × 0.14	0.24 × 0.13 × 0.11	0.26 × 0.08 × 0.06
Data collection					
Diffractometer	KappaCCD	KappaCCD	KappaCCD	KappaCCD	KappaCCD
Data collection method	φ scans, and ω scans with κ offsets	φ scans, and ω scans with κ offsets	φ scans, and ω scans with κ offsets	φ scans, and ω scans with κ offsets	φ scans, and ω scans with κ offsets
Absorption correction	Multi-scan	Multi-scan	Multi-scan	Multi-scan	Multi-scan
T_{min}	0.7936	0.8640	0.8711	0.8184	0.8688
T_{max}	0.8792	0.9953	0.8976	0.9104	0.9674
No. of measured, independent and observed reflections	15103, 3166, 2798	7460, 2910, 2244	10444, 4458, 2882	10111, 4096, 3141	8932, 3268, 2589
Criterion for observed reflections	$I > 2\sigma(I)$	$I > 2\sigma(I)$	$I > 2\sigma(I)$	$I > 2\sigma(I)$	$I > 2\sigma(I)$
R_{int}	0.037	0.051	0.047	0.039	0.052
θ_{max} (°)	27.50	25.06	27.47	27.50	27.57
Range of h, k, l	$0 \rightarrow h \rightarrow 40$ $0 \rightarrow k \rightarrow 10$ $-15 \rightarrow l \rightarrow 14$	$0 \rightarrow h \rightarrow 8$ $-12 \rightarrow k \rightarrow 12$ $-13 \rightarrow l \rightarrow 12$	$0 \rightarrow h \rightarrow 9$ $-11 \rightarrow k \rightarrow 0$ $-39 \rightarrow l \rightarrow 37$	$0 \rightarrow h \rightarrow 9$ $-13 \rightarrow k \rightarrow 13$ $-16 \rightarrow l \rightarrow 16$	$0 \rightarrow h \rightarrow 8$ $-12 \rightarrow k \rightarrow 12$ $-15 \rightarrow l \rightarrow 15$
Refinement					
Refinement on	F^2	F^2	F^2	F^2	F^2
$R[F^2 > 2\sigma(F^2)]$, $wR(F^2)$, S	0.0278, 0.0715, 1.034	0.04, 0.0972, 1.029	0.0466, 0.0998, 1.03	0.038, 0.0888, 1.029	0.0436, 0.0909, 1.068
No. of reflections and parameters used in refinement	3166, 185	2910, 229	4458, 279	4096, 264	3268, 162
H-atom treatment	H-atom parameters constrained	H-atom parameters constrained	H-atom parameters constrained	H-atom parameters constrained	H-atom parameters constrained
Weighting scheme	$w = 1/[\sigma^2(F_o^2) + (0.0222P)^2 + 2.8956P]$ where $P = (F_o^2 + 2F_c^2)/3$	$w = 1/[\sigma^2(F_o^2) + 0.1851P]$ where $P = (F_o^2 + 2F_c^2)/3$	$w = 1/[\sigma^2(F_o^2) + (0.0295P)^2 + 0.1109P]$ where $P = (F_o^2 + 2F_c^2)/3$	$w = 1/[\sigma^2(F_o^2) + 0.5387P]$ where $P = (F_o^2 + 2F_c^2)/3$	$w = 1/[\sigma^2(F_o^2) + 0.2558P]$ where $P = (F_o^2 + 2F_c^2)/3$
$(\Delta/\sigma)_{max}$	<0.001	<0.001	0.001	<0.001	<0.001
$\Delta\rho_{max}$, $\Delta\rho_{min}$ (e Å^{-3})	0.365, −0.404	0.306, −0.334	0.394, −0.372	0.518, −0.315	0.242, −0.432
Extinction method	*SHELXL*	*SHELXL*	None	None	None
Extinction coefficient	0.0014 (2)	0.006 (2)	–	–	–

	(6)	(7)	(8)	(9)
Crystal data				
Chemical formula	$(C_5H_{12}N)[Fe(C_6H_4O_2)(C_6H_5O_2)]$	$(C_{12}H_{24}N)_2[Fe(C_6H_4O_2)(C_6H_5O_2)]_2\cdot C_4H_8O$	$(C_6H_{21}N_4)_2[Fe(C_6H_4O_2)_2]_3$	$(C_8H_{12}NO)_2[Fe(C_6H_4O_2)_2]$
Chemical formula weight	359.2	982.83	1114.64	548.41
Cell setting, space group	Monoclinic, $P2_1/c$	Triclinic, $P\bar{1}$	Triclinic, $P\bar{1}$	Triclinic, $P\bar{1}$
a, b, c (Å)	5.9880 (3), 19.4750 (12), 13.4340 (9)	10.3588 (2), 11.9612 (2), 22.7731 (5)	9.7360 (19), 13.661 (3), 22.855 (5)	12.6828 (4), 13.2119 (4), 14.3107 (4)

Table 1 (continued)

	(6)	(7)	(8)	(9)
α, β, γ (°)	90, 99.058 (3), 90	74.9690 (8), 78.0660 (8), 64.459 (1)	97.51 (3), 99.09 (3), 91.11 (3)	64.4870 (14), 68.4460 (12), 72.2550 (15)
V (Å^3)	1547.09 (16)	2444.18 (8)	2973.3 (10)	1981.88 (10)
Z	4	2	2	3
D_x (Mg m^{-3})	1.542	1.335	1.245	1.378
Radiation type	Mo $K\alpha$	Mo $K\alpha$	Mo $K\alpha$	Mo $K\alpha$
No. of reflections for cell parameters	2442	9949	7818	8309
θ range (°)	3.45–25.08	2.67–27.46	2.55–25.03	2.55–27.48
μ (mm^{-1})	0.995	0.651	0.781	0.616
Temperature (K)	150 (2)	150 (2)	150 (2)	150 (2)
Crystal form, colour	Needle, orange	Plate, colourless	Block, orange	Block, colourless
Crystal size (mm)	0.30 × 0.15 × 0.12	0.26 × 0.20 × 0.08	0.35 × 0.30 × 0.28	0.08 × 0.06 × 0.04
Data collection				
Diffractometer	KappaCCD	KappaCCD	KappaCCD	KappaCCD
Data collection method	φ scans, and ω scans with κ offsets	φ scans, and ω scans with κ offsets	φ scans, and ω scans with κ offsets	φ scans, and ω scans with κ offsets
Absorption correction	Multi-scan	Multi-scan	Multi-scan	Multi-scan
T_{min}	0.7545	0.8490	0.7717	0.9524
T_{max}	0.8899	0.9498	0.8110	0.9758
No. of measured, independent and observed reflections	7828, 2694, 1926	27832, 11044, 8558	20136, 10158, 8024	24541, 8904, 6112
Criterion for observed reflections	$I > 2\sigma(I)$	$I > 2\sigma(I)$	$I > 2\sigma(I)$	$I > 2\sigma(I)$
R_{int}	0.068	0.041	0.039	0.081
θ_{max} (°)	25.08	27.46	25.09	27.43
Range of h, k, l	$0 \rightarrow h \rightarrow 7$ $0 \rightarrow k \rightarrow 23$ $-16 \rightarrow l \rightarrow 15$	$0 \rightarrow h \rightarrow 13$ $-13 \rightarrow k \rightarrow 15$ $-28 \rightarrow l \rightarrow 29$	$0 \rightarrow h \rightarrow 11$ $-16 \rightarrow k \rightarrow 16$ $-27 \rightarrow l \rightarrow 26$	$0 \rightarrow h \rightarrow 16$ $-15 \rightarrow k \rightarrow 17$ $-16 \rightarrow l \rightarrow 18$
Refinement				
Refinement on	F^2	F^2	F^2	F^2
$R[F^2 > 2\sigma(F^2)]$, $wR(F^2)$, S	0.045, 0.1074, 1.051	0.0407, 0.1022, 1.032	0.0624, 0.1604, 1.093	0.0563, 0.1504, 1.033
No. of reflections and parameters used in refinement	2694, 210	11044, 603	10158, 647	8904, 508
H-atom treatment	H-atom parameters constrained	H-atom parameters constrained	H-atom parameters constrained	H-atom parameters constrained
Weighting scheme	$w = 1/[\sigma^2(F_o^2) + (0.0363P)^2 + 0.1390P]$ where $P = (F_o^2 + 2F_c^2)/3$	$w = 1/[\sigma^2(F_o^2) + (0.0239P)^2 + 1.6289P]$ where $P = (F_o^2 + 2F_c^2)/3$	$w = 1/[\sigma^2(F_o^2) + (0.0523P)^2 + 7.1596P]$ where $P = (F_o^2 + 2F_c^2)/3$	$w = 1/[\sigma^2(F_o^2) + (0.0455P)^2 + 0.6258P]$ where $P = (F_o^2 + 2F_c^2)/3$
$(\Delta/\sigma)_{max}$	0.001	0.001	0.001	0.001
$\Delta\rho_{max}$, $\Delta\rho_{min}$ (e Å^{-3})	0.562, −0.664	0.569, −0.578	0.655, −0.66	0.333, −0.533
Extinction method	None	None	*SHELXL*	None
Extinction coefficient	–	–	0.013 (1)	–

Computer programs used: *PRPKAPPA* (Ferguson, 1999), *KappaCCD* (Nonius, 1997), *DENZO-SMN* (Otwinowski & Minor, 1997), *SHELXL*97 (Sheldrick, 1997*a*), *SHELXS*97 (Sheldrick, 1997*b*), *PLATON* (Spek, 2002).

tures were solved by direct methods and refined with all data on F^2. A weighting scheme based on $P = (F_o^2 + 2F_c^2)/3$ was employed in order to reduce statistical bias (Wilson, 1976). In (2) there is partial transfer of H from O to N, and this disorder was modelled for each O···H···N interaction with two H sites, each having 0.5 occupancy, one adjacent to O and one adjacent to N. In (6) there is similar disorder of H between two carboxylate O atoms in different anions, and again this was modelled using two sites, one adjacent to each O, with 0.5 occupancy for each. All other H atoms were fully ordered and all were included in the refinements as riding atoms with O—H = 0.84 Å, N—H = 0.88–0.93 Å and C—H = 0.93–1.00 Å. The refined structure of (8) was found to contain significant void space, including a large void centred at (0, 0, $\frac{1}{2}$) and having volume 634 Å^3, together with two much smaller voids each of volume 30 Å^3; together these voids represent some 23% of the unit-cell volume. Since no coherent molecular fragments could be identified at these sites, the *SQUEEZE* option in *PLATON* (Spek, 2002) was employed, and this indicated that the voids account for only 27 electrons per unit cell, corresponding to 0.675 molecules of tetrahydrofuran solvent per unit cell.

Supramolecular analyses were made and the diagrams were prepared with the aid of *PLATON* (Spek, 2002). Hydrogen-bonding details are given in Table 2 and details of the molecular conformations in Tables 3 and 4.[1] Figs. 1–29 show the molecular aggregates, with the atom-labelling schemes and aspects of the supramolecular structures.

[1] Lists of atomic coordinates, anisotropic displacement parameters, geometric parameters and structure factors have been deposited with the IUCr (Reference: NA0136). Services for accessing these data are described at the back of the journal.

Table 2
Hydrogen-bond parameters (Å, °).

	D—H···A	H···A	D···A	D—H···A
(1)	O11—H11···O22^{i}	1.74	2.573 (2)	172
	N1—H1A···O21^{ii}	1.85	2.752 (2)	168
	N1—H1B···O21	2.38	3.104 (2)	135
	N1—H1B···O22	1.95	2.792 (2)	152
	C2—H2B···O12^{ii}	2.46	3.420 (2)	168
	C22—H22···O11^{iii}	2.42	3.236 (2)	143
(2)	N1—H1†···O11	1.65	2.580 (3)	176
	N2—H2†···O21^{iv}	1.62	2.552 (3)	177
	O11—H11†···N1	1.74	2.580 (3)	178
	O21—H21†···N2^{v}	1.72	2.552 (3)	174
	C31—H31B···O22^{vi}	2.47	3.373 (4)	152
	C52—H52B···O12^{vii}	2.33	3.262 (4)	157
(3)	O5—H51···O11	1.86 (2)	2.692 (3)	160 (3)
	O5—H52···O12^{viii}	1.86 (2)	2.715 (3)	175 (3)
	N34—H34A···O22^{ix}	1.84	2.752 (3)	170
	N34—H34B···O11	1.93	2.763 (3)	150
	N44—H44A···O5	1.92	2.817 (3)	166
	N44—H44B···O22	1.82	2.706 (3)	162
	C45—H45B···O41^{x}	2.41	3.312 (4)	151
(4)	O11—H11···N31	1.83	2.674 (2)	179
	O21—H21···N41^{xi}	1.79	2.629 (2)	177
	C46—H46···O12^{xii}	2.30	3.232 (3)	169
(5)	N1—H1A···O2^{xiii}	1.88	2.767 (2)	165
	N1—H1B···O2^{xiv}	1.85	2.721 (2)	159
	N1—H1C···O1	1.79	2.689 (2)	168
(6)	N1—H1A···O12	1.89	2.746 (4)	153
	N1—H1B···O11^{xiv}	2.44	3.074 (4)	126‡
	N1—H1B···O22^{xv}	2.06	2.854 (4)	144‡
	O11—H11†···O21^{xvi}	1.63	2.459 (4)	168
	O21—H21†···O11^{xvii}	1.62	2.459 (4)	176
(7)	O12—H12···O41	1.76	2.600 (2)	174
	O32—H32···O21^{xiv}	1.76	2.587 (2)	170
	N1—H1A···O42^{x}	1.82	2.720 (2)	166
	N1—H1B···O41	1.93	2.810 (2)	161
	N2—H2A···O21	1.91	2.822 (2)	170
	N2—H2B···O22^{xviii}	1.86	2.751 (2)	162
	C44—H44···O11^{xiv}	2.47	3.418 (3)	173
	C61—H61···O11	2.27	3.241 (2)	164
(8)	N11—H11A···O42	2.02	2.902 (5)	162
	N11—H11B···O32^{xix}	1.93	2.819 (5)	164
	N11—H11C···O31^{xiv}	1.82	2.720 (5)	168
	N12—H12A···O42	1.95	2.834 (5)	163
	N12—H12B···O32	1.80	2.699 (5)	168
	N12—H12C···O41^{xix}	1.84	2.727 (5)	165
	N13—H13A···O42	1.97	2.869 (5)	170
	N13—H13B···O62	1.80	2.704 (5)	171
	N13—H13C···O22	1.83	2.711 (6)	163
	N21—H21A···O21	1.80	2.704 (6)	172
	N21—H21B···O61	1.90	2.770 (5)	158
	N21—H21C···O51^{xx}	2.05	2.933 (5)	162
	N22—H22A···O12^{xxi}	1.86	2.722 (5)	158
	N22—H22B···O12	1.88	2.756 (5)	161
	N22—H22C···O51^{xx}	1.94	2.822 (5)	161
	N23—H23A···O52	1.82	2.697 (5)	161
	N23—H23B···O61^{xx}	1.83	2.705 (5)	162
	N23—H23C···O51^{xx}	2.02	2.887 (5)	158
(9)	N4—H4A···O22	1.85	2.734 (4)	162
	N4—H4B···O12^{xx}	1.86	2.742 (4)	162
	N4—H4C···O32^{xxii}	1.90	2.801 (3)	171
	N5—H5A···O31^{vii}	1.88	2.749 (3)	158
	N5—H5B···O12^{xix}	1.83	2.726 (3)	168
	N5—H5C···O5^{vii}	2.18	2.968 (3)	145
	N6—H6A···O32^{vi}	2.11	3.009 (4)	170

Table 2 (continued)

D—H···A	H···A	D···A	D—H···A
N6—H6B···O11^{xxiii}	1.85	2.731 (3)	164
N6—H6C···O21^{i}	2.10	2.941 (3)	154
O4—H4···O11	1.85	2.679 (4)	170
O5—H5···O21	1.75	2.577 (3)	166
O6—H6···O31	1.87	2.669 (3)	164

Symmetry codes: (i) $x, -1+y, z$; (ii) $\frac{1}{2}-x, \frac{1}{2}+y, \frac{1}{2}-z$; (iii) $x, 1+y, z$; (iv) $-1+x, y, 1+z$; (v) $1+x, y, -1+z$; (vi) $-x, -y, -z$; (vii) $-x, 1-y, 1-z$; (viii) $-x, 1-y, -z$; (ix) $-1+x, y, z$; (x) $1-x, -y, -z$; (xi) $-2+x, y, 1+z$; (xii) $2-x, -y, -z$; (xiii) $2-x, 2-y, 1-z$; (xiv) $1+x, y, z$; (xv) $2-x, -\frac{1}{2}+y, \frac{1}{2}-z$; (xvi) $1-x, -\frac{1}{2}+y, \frac{1}{2}-z$; (xvii) $1-x, \frac{1}{2}+y, \frac{1}{2}-z$; (xviii) $-1-x, 1-y, 1-z$; (xix) $1-x, 1-y, 1-z$; (xx) $1-x, 1-y, -z$; (xxi) $1-x, 2-y, -z$; (xxii) $-x, 1-y, -z$; (xxiii) $-1+x, -1+y, z$. † Disordered H atoms, occupancy 0.5. ‡ Three-centre N—H···$(O)_2$ system: sum of angles at H1B = 360°.

Table 3
Selected torsional angles in ferrocene components (°).

Compound	Charge on ferrocene component	Mean value of Cpn—$Cg(p)$—$Cg(q)$—Cqn†		m†
(1)	1−	$p = 1, q = 2$	71.7	2
(2)	‡	$p = 1, q = 2$	−178.8	5
(3)	2−	$p = 1, q = 2$	−7.4	0
(4)	0	$p = 1, q = 2$	176.5	5
(5)	2−	$p = 1, q = 1$§	180.0	5
(6)	1−	$p = 1, q = 2$	−141.5	4
(7)	1−	$p = 1, q = 2$	147.8	4
		$p = 3, q = 4$	148.2	4
(8)	2−	$p = 1, q = 2$	−112.4	3
		$p = 3, q = 4$	−51.4	1
		$p = 5, q = 6$	−52.8	1
(9)	2−	$p = 1, q = 1$§	180.0	5
		$p = 2, q = 3$	−4.5	0

† $Cg(p)$, $Cg(q)$ are centroids of rings Cp1–Cp5 and Cq1–Cq5; m = (mean torsional angle)/36 (see §3.4.1). ‡ Partial transfer of H from O to N (see §3.1.2). § Symmetry position $1-x, 1-y, 1-z$.

3. Results and discussion

3.1. Hard hydrogen bonds produce one-dimensional structures

3.1.1. Soft hydrogen bonds do not influence dimensionality. *Dimethylammonium ferrocene-1-carboxylic acid 1′-carboxylate(1−), (1)*. The 1:1 adduct (1) formed between ferrocene-1,1′-dicarboxylic acid and dimethylamine is a salt $Me_2NH_2^+.[Fe(C_5H_4COO)(C_5H_4COOH)]^-$ (Fig. 1) and the supramolecular aggregation takes the form of chains of fused rings. The anions alone form $C(8)$ chains by translation along the [010] direction and pairs of these chains, related by the 2_1 screw axes along [101], are linked by the cations (Fig. 2). Hydroxyl O11 at (x, y, z) acts as hydrogen-bond donor to carboxylate O22 at (x, $-1+y$, z); atom N1 in the cation at (x, y, z) acts as hydrogen-bond donor *via* H1B to both O21 and O22 within the asymmetric unit, generating a rather asymmetric three-centre system, and *via* H1A to O21 at ($\frac{1}{2}-x$, $\frac{1}{2}+y$, $\frac{1}{2}-z$). Propagation of the hydrogen bonds produces a chain of fused $R_1^2(4)$ and $R_5^3(16)$ rings, generated by the screw axis along ($\frac{1}{4}$, y, $\frac{1}{4}$). Another parallel chain is generated by the 2_1 axis along ($\frac{3}{4}$, y, $\frac{1}{4}$), while two antiparallel chains lie along ($\frac{1}{4}$, $-y$, $\frac{3}{4}$) and ($\frac{3}{4}$, $-y$, $\frac{3}{4}$) (Fig. 3), but there are neither hydrogen bonds nor $\pi\cdots\pi$ stacking interactions between adjacent chains. The only significant C—H$\cdots$O hydrogen bonds (H$\cdots$O < 2.50 Å, C$\cdots$O < 3.50 Å, C—H$\cdots$O > 130°) (Table 2) both lie within the chain of fused rings and hence have no influence on the overall dimensionality of the supramolecular structure, which is thus strictly one-dimensional.

3.1.2. Soft hydrogen bonds produce two-dimensional structures. *1,4-Diazabicyclo[2.2.2]octane–ferrocene-1,1′-dicarboxylic acid (1/1), (2)*. In (2), the 1:1 adduct of ferrocene-1,1′-dicarboxylic acid and 1,4-diazabicyclo[2.2.2]octane, both molecular components lie in general positions (Fig. 4). The acidic H of each carboxyl unit is partially transferred from O11 and O21 to the adjacent N atoms. In both of the independent O$\cdots$H$\cdots$N units, the disorder was best modelled by two H-atom sites with 0.50 occupancy, one adjacent to O and the other adjacent to N. For any given O$\cdots$N pair of this type, only one H site is occupied at any instant, although the H may tunnel between the alternative sites; however, there is no necessary correlation between the

Table 4
Selected torsional and dihedral angles in amine components (°).

(2)	N1—C31—C32—N2	3.1 (3)		
	N1—C41—C42—N2	2.1 (3)		
	N1—C51—C52—N2	3.4 (3)		
(4)	(N31, C32—C36)^(N41, C42—C46)	27.6 (2)		
(5)	N1—C2—C3—C4	−177.7 (2)	C4—C5—C6—C7	179.4 (2)
	C2—C3—C4—C5	179.2 (2)	C5—C6—C7—C8	177.0 (2)
	C3—C4—C5—C6	−178.3 (2)	C6—C7—C8—C9	−179.7 (2)
(8)	N1—C71—C72—N11	65.8 (5)	N2—C81—C82—N21	−67.7 (5)
	N1—C73—C74—N12	63.4 (6)	N2—C83—C84—N22	−69.4 (5)
	N1—C75—C76—N13	69.3 (5)	N2—C85—C86—N23	−60.3 (4)
(9)	C44—C47—C48—N4	169.8 (3)	C43—C44—C47—C48	111.4 (4)
	C54—C57—C58—N5	−54.5 (4)	C53—C54—C57—C58	−73.7 (4)
	C64—C67—C68—N6	−173.4 (3)	C63—C64—C67—C68	−110.0 (4)

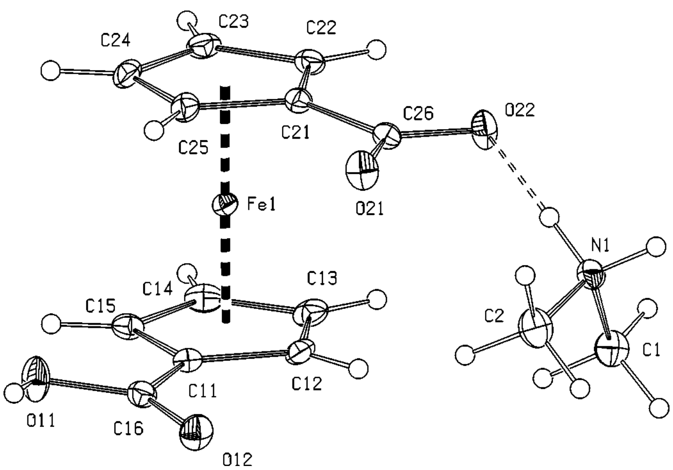

Figure 1
The asymmetric unit of (1), showing the atom-labelling scheme. Displacement ellipsoids are drawn at the 30% probability level.

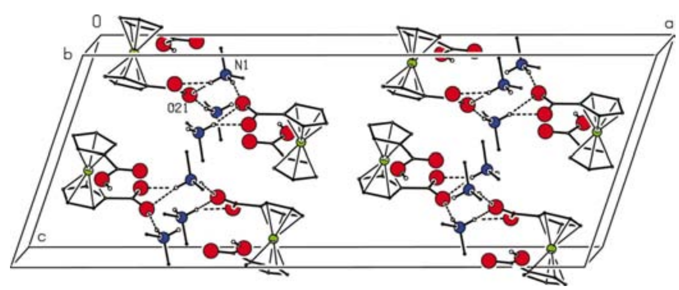

Figure 3
Projection of part of the crystal structure of (1), showing the four independent chains running through the unit cell. For the sake of clarity, H atoms bonded to C are omitted.

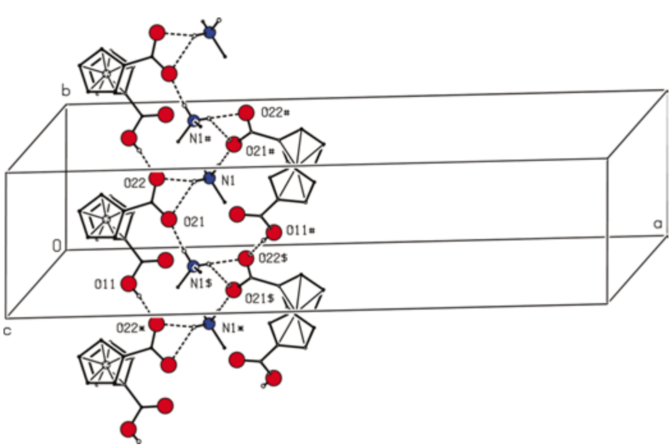

Figure 2
Part of the crystal structure of (1), showing the formation of a chain of fused rings along [010]. For the sake of clarity, H atoms bonded to C are omitted. The atoms marked with a star (*), hash (#) or dollar sign ($) are at the symmetry positions (x, $-1 + y$, z), ($\frac{1}{2} - x$, $\frac{1}{2} + y$, $\frac{1}{2} - z$) and ($\frac{1}{2} - x$, $-\frac{1}{2} + y$, $\frac{1}{2} - z$), respectively.

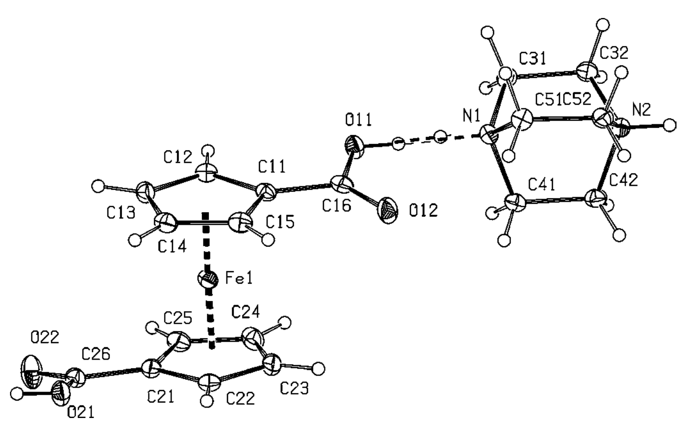

Figure 4
The molecular components of (2), showing the atom-labelling scheme: the H-atom sites adjacent to N and O all have 0.50 occupancy. Displacement ellipsoids are drawn at the 30% probability level.

H site occupancies in different O$\cdots$H$\cdots$N units. Regardless of the site occupancies at the local level, the net effect is to generate hard hydrogen bonds, of O—H$\cdots$N and N—H$\cdots$O types, between the two molecular components such that chains are formed in which the two components alternate.

There is a hydrogen bond between O11 and N1 within the asymmetric unit and another between O21 at (x, y, z) and N2 at ($1 + x$, y, $-1 + z$). In this manner, a $C_2^2(13)$ chain is generated that runs parallel to the [10$\bar{1}$] direction. Two such chains, antiparallel to one another and related by the centres of inversion, run through each unit cell, and each chain is linked to two others by two independent C—H$\cdots$O hydrogen bonds. Atom C31 in the DABCO unit at (x, y, z) acts as donor, *via* H31*B*, to carboxyl O22 at ($-x$, $-y$, $-z$), and propagation of this hydrogen bond links pairs of chains *via* a series of fused centrosymmetric $R_4^4(16)$ and $R_4^4(22)$ rings (Fig. 5). Similarly, C52 at (x, y, z) acts as donor, *via* H52*B*, to O12 at ($-x$, $1 - y$, $1 - z$), so generating a second sequence of $R_4^4(16)$ and $R_4^4(22)$ rings, similar to the first sequence but distinct from it (Fig. 5).

The combined effect of the two C—H$\cdots$O hydrogen bonds is to link the [10$\bar{1}$] chains into a (10$\bar{1}$) sheet: in this case there are no $\pi\cdots\pi$ stacking interactions linking adjacent sheets.

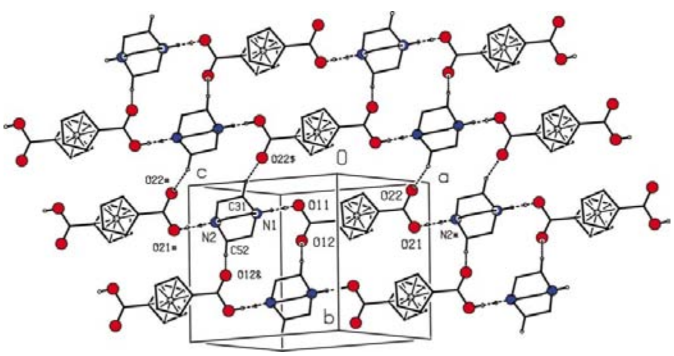

Figure 5
Part of the crystal structure of (2), showing chains formed by the hard hydrogen bonds linked into sheets by the soft hydrogen bonds. For the sake of clarity, H atoms not involved in the hydrogen bonding are omitted. The atoms marked with a star (*), hash (#), dollar sign ($) or ampersand (&) are at the symmetry positions ($1 + x$, y, $-1 + z$), ($-1 + x$, y, $1 + z$), ($1 - x$, $-y$, $- z$) and ($-x$, $1 - y$, $1 - z$), respectively.

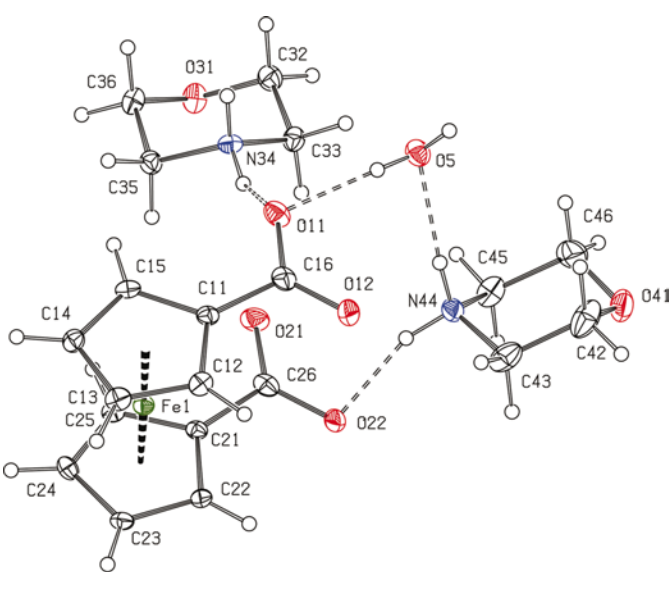

Figure 6
The molecular components of (3), showing the atom-labelling scheme. Displacement ellipsoids are drawn at the 30% probability level.

Bis[morpholinium(1+)] ferrocene-1,1′-dicarboxylate(2−) monohydrate, (3). Ferrocene-1,1′-dicarboxylic acid forms a hydrated salt with morpholine, $O(CH_2CH_2)_2NH$, in which both carboxyl H atoms are transferred from the acid to the base, giving $2[O(CH_2CH_2)_2NH_2^+].[Fe(C_5H_4COO)_2]^{2-}.H_2O$, (3) (a salt). The four independent components all lie in general positions and they are linked by six hydrogen bonds, two of O—H$\cdots$O type and four of N—H$\cdots$O type (Table 2). However, it is possible to select an asymmetric unit (Fig. 6) that encompasses four of the hydrogen bonds, leaving just two hard hydrogen bonds to link these four-component aggregates into molecular ladders.

The cations of type 1 (containing N34) and the anions together form chains by translation along the [100] direction, and antiparallel pairs of these chains form the uprights of the molecular ladder, with paired water molecules forming the rungs. Atom N34 at (x, y, z) acts as hydrogen-bond donor *via* H34*B* to O11 within the asymmetric unit (Fig. 6) and *via* H34*A* to O22 at ($-1 + x$, y, z), so generating by translation a $C_2^2(10)$ chain (Fig. 7). The water O5 at (x, y, z) acts as donor *via* H51 to O11 within the asymmetric unit and *via* H52 to O12 at ($-x$, $1 - y$, $-z$), so generating a centrosymmetric $R_4^4(12)$ ring (Fig. 7). With the $R_4^4(12)$ rings centred at (n, $\frac{1}{2}$, 0) (n = zero or integer) acting as the rungs of the ladder, there are $R_8^6(28)$ rings centred at ($n + \frac{1}{2}$, $\frac{1}{2}$, 0) (n = zero or integer) between the rungs. Two such ladders run through each unit cell, one in the domain $-0.24 < z < 0.24$ and the other in the domain $0.26 < z < 0.74$.

Within each domain, the ladders are linked by a single C—H$\cdots$O hydrogen bond. Atom C45 at (x, y, z) is adjacent to

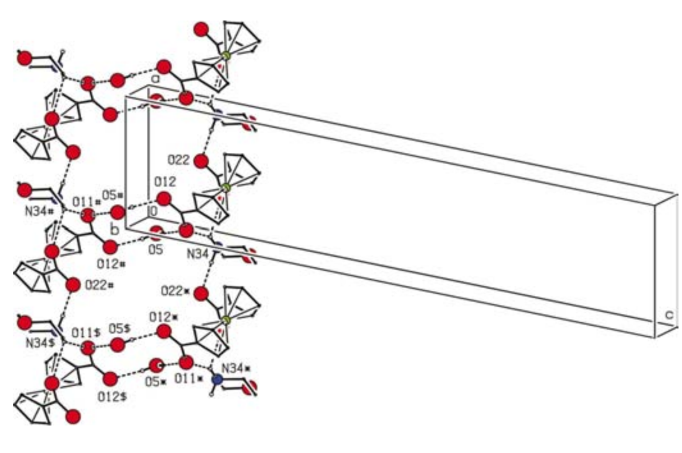

Figure 7
Part of the crystal structure of (3), showing the formation of a molecular ladder along [100]. For the sake of clarity, H atoms not involved in the hydrogen bonding are omitted. The atoms marked with a star (*), hash (#) or dollar sign ($) are at the symmetry positions ($-1 + x$, y, z), ($-x$, $1 - y$, $-z$) and ($-1 - x$, $1 - y$, $-z$), respectively.

the cationic N44 in the type 2 cation and it lies in the molecular ladder along $(x, \frac{1}{2}, 0)$: this C acts as hydrogen-bond donor, *via* H45*B*, to the morpholine O41 at $(1 - x, -y, -z)$, which lies in the adjacent molecular ladder along $(x, -\frac{1}{2}, 0)$, so forming an $R_2^2(8)$ ring (Fig. 8). Propagation of this hydrogen bond thus links all the ladders in the domain $-0.24 < z < 0.24$ into a single continuous sheet and all of those in the domain $0.26 < z < 0.74$ into a second such sheet, but there are no specific interactions between adjacent sheets.

4,4′-Bipyridyl–ferrocene-1,1′-dicarboxylic acid (1/1), (4). In (4), both the ferrocenedicarboxylic acid and the 4,4′-bipyridyl molecules lie in general positions, although both could, in principle, lie across a centre of inversion, a twofold rotation axis or a mirror plane. The acid acts as a twofold donor in O—H···N hydrogen bonds and the bipyridyl acts as a twofold acceptor. The basic structural motif generated by the hard (Braga *et al.*, 1995) O—H···N hydrogen bonds is chain formation. Within the asymmetric unit, atom O11 acts as hydrogen-bond donor to N31 (Fig. 9), and in addition O21 at (x, y, z) acts as donor to N41 at $(-2 + x, y, 1 + z)$: propagation of these two hydrogen bonds by translation thus generates a $C_2^2(17)$ chain running parallel to the $[20\bar{1}]$ direction (Fig. 10). Two such chains, related to one another by the centres of inversion and thus running antiparallel to one another, pass through each unit cell.

Each chain is linked to two adjacent chains by soft C—H···O hydrogen bonds, so generating a sheet structure (Fig. 10). Atom C46 in the bipyridyl unit at (x, y, z) acts as donor to O12 at $(2 - x, -y, -z)$, while C46 at $(2 - x, -y, -z)$ in turn acts as donor to O12 at (x, y, z). This C—H···O hydrogen bond thus effects a pairwise linking of antiparallel chains *via* a series of fused and centrosymmetric rings in which $R_4^4(22)$ and $R_4^4(24)$ rings alternate (Fig. 10). In addition, C36 at (x, y, z) acts as donor to O22 at $(1 - x, 1 - y, 1 - z)$, and propagation of this hydrogen bond generates a second sequence of fused centrosymmetric rings, also of $R_4^4(22)$ and $R_4^4(24)$ types but distinct from the first series. In this manner, the two C—H···O hydrogen bonds link all the $[20\bar{1}]$ chains into sheets parallel to the $(2\bar{2}1)$ plane.

These sheets are themselves weakly linked by aromatic $\pi\cdots\pi$ stacking interactions between ring C11–C15 of the acid component and the ring containing N31 in the bipyridyl component. Ring C11–C15 in the acid at (x, y, z) makes an angle of only *ca* 7.4° with the N31, C32–C36 ring at $(-1 + x, y, z)$, a component of the adjacent sheet: the distance between ring centroids is 3.662 (2) Å and the centroid offset distance is 1.574 (2) Å.

3.2. Hard hydrogen bonds produce two-dimensional structures

3.2.1. Soft hydrogen bonds are absent. *Bis[octylammonium(1+)] ferrocene-1,1′-dicarboxylate(2−), (5)*. The 2:1 adduct (5) formed between octylamine and ferrocene-1,1′-dicarboxylic acid is a salt, $2(C_8H_{17}NH_3^+).[Fe(C_5H_4COO)_2]^{2-}$. The anion lies across a centre of inversion in space group $P\bar{1}$, chosen for the sake of convenience as that at $(\frac{1}{2}, \frac{1}{2}, \frac{1}{2})$, so that the cyclopentadienyl rings are precisely staggered. The cation, which adopts the all-*trans* extended chain conformation, lies in a general position. The ions are linked into sheets parallel to (001), whose formation can be analysed readily in terms of two substructures in the form of molecular ladders parallel to [100] and [010].

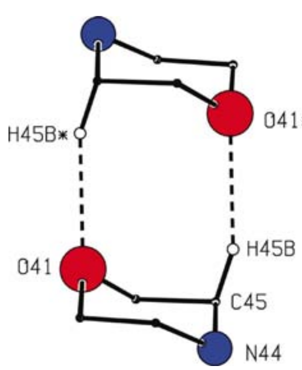

Figure 8
Part of the crystal structure of (3), showing the $R_2^2(8)$ motif linking adjacent molecular ladders. The atoms marked with a star (*) are at the symmetry position $(1 - x, -y, -z)$.

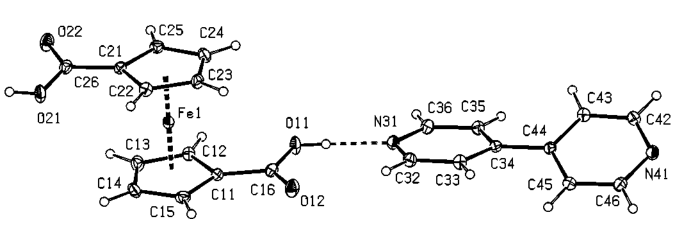

Figure 9
The molecular components of (4), showing the atom-labelling scheme. Displacement ellipsoids are drawn at the 30% probability level.

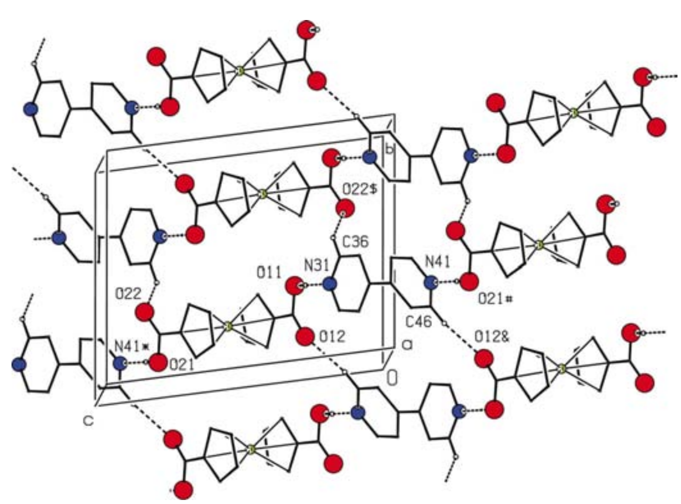

Figure 10
Part of the crystal structure of (4), showing chains formed by the hard hydrogen bonds linked into sheets by the soft hydrogen bonds. For the sake of clarity, H atoms not involved in the hydrogen bonding are omitted. The atoms marked with a star (*), hash (#), dollar sign ($) or ampersand (&) are at the symmetry positions $(-2 + x, y, 1 + z)$, $(2 + x, y, -1 + z)$, $(1 - x, 1 - y, 1 - z)$ and $(2 - x, -y, -z)$, respectively.

Within the asymmetric unit (Fig. 11), ammonium N1 acts as hydrogen-bond donor, *via* H1*C*, to carboxylate O1; similarly, N1 at $(1-x, 1-y, 1-z)$ acts as donor to O1 at $(1-x, 1-y, 1-z)$ within the same anion centred at $(\frac{1}{2}, \frac{1}{2}, \frac{1}{2})$, so forming a three-ion aggregate, cation–anion–cation. At the same time, N1 at (x, y, z) also acts as donor, this time *via* H1*B*, to O2 at $(1+x, y, z)$, so generating by translation a $C_2^2(6)$ chain running parallel to [100]. The action of the centres of inversion at $(n+\frac{1}{2}, \frac{1}{2}, \frac{1}{2})$ (n = zero or integer) thus generates a molecular ladder parallel to [100] (Fig. 12) in which the uprights are formed by an antiparallel pair of $C_2^2(6)$ chains and the rungs are formed by the anions. Between the rungs, there are $R_4^4(20)$ rings centred at $(n, \frac{1}{2}, \frac{1}{2})$ (n = zero or integer).

Finally, N1 at (x, y, z) also acts as hydrogen-bond donor, this time *via* H1*A*, to O2 at $(2-x, 2-y, 1-z)$, so generating another $R_4^4(20)$ ring centred at $(1, 1, \frac{1}{2})$: N1 at (x, y, z) lies in the molecular ladder along $(x, \frac{1}{2}, \frac{1}{2})$, while O2 at $(2-x, 2-y, 1-z)$ lies in the ladder along $(x, \frac{3}{2}, \frac{1}{2})$. Hence propagation of this hydrogen bond generates a second molecular ladder, entirely similar to the first but running parallel to [010]. The combination of the ladders along [100] and [010] generates the (001) sheet, just one of which passes through each unit cell. There are no direction-specific interactions of any kind between adjacent sheets.

3.2.2. Soft hydrogen bonds do not influence dimensionality. *Piperidinium(1+) ferrocene-1-carboxylic acid 1′-carboxylate(1−), (6)*. In (6) (Fig. 13), the amine is fully protonated to form the $C_5H_{10}NH_2^+$ cation, so the resultant charge per ferrocene unit is 1−. The monoanions are linked into spiral chains by O—H···O hydrogen bonds, but within each such hydrogen bond the H is disordered over two sites, one adjacent to each O, which have equal occupancies (Table 2). While it is possible that within each individual O—H···O unit the H are mobile between the two sites, there is no necessary correlation between the occupancies in adjacent hydrogen bonds. While the average charge per ferrocene is 1−, there may be present at any instant both neutral acid molecules and dianions.

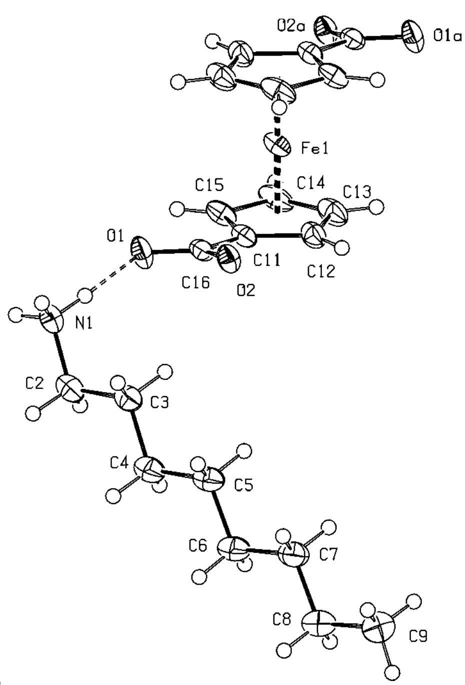

Figure 11
The molecular components of (5), showing the atom-labelling scheme. Displacement ellipsoids are drawn at the 30% probability level. The atoms marked ‘a’ are at the symmetry position $(1-x, 1-y, 1-z)$.

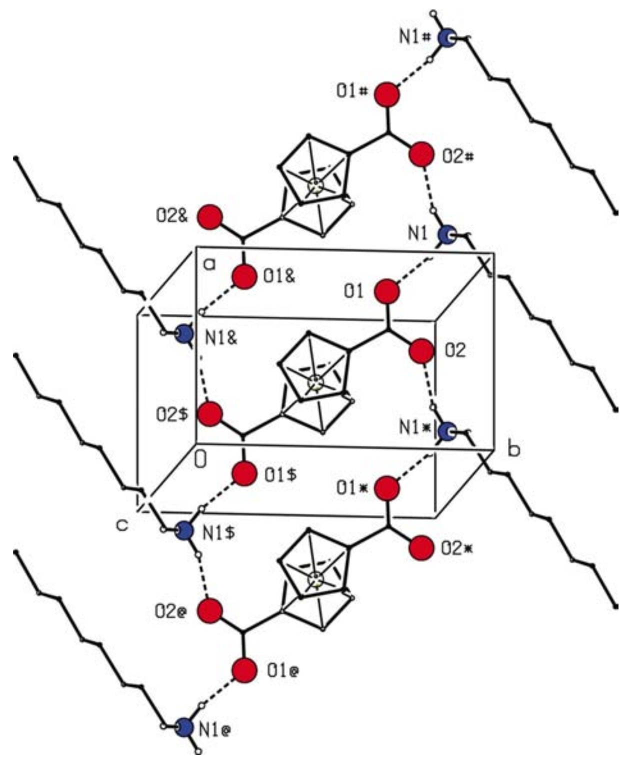

Figure 12
Part of the crystal structure of (5), showing the formation of a molecular ladder along [100]. For the sake of clarity, H atoms not involved in the hydrogen bonding are omitted. The atoms marked with a star (*), hash (#), dollar sign ($), ampersand (&) or at sign (@) are at the symmetry positions $(-1+x, y, z)$, $(1+x, y, z)$, $(1-x, 1-y, 1-z)$, $(2-x, 1-y, 1-z)$ and $(-x, 1-y, 1-z)$, respectively.

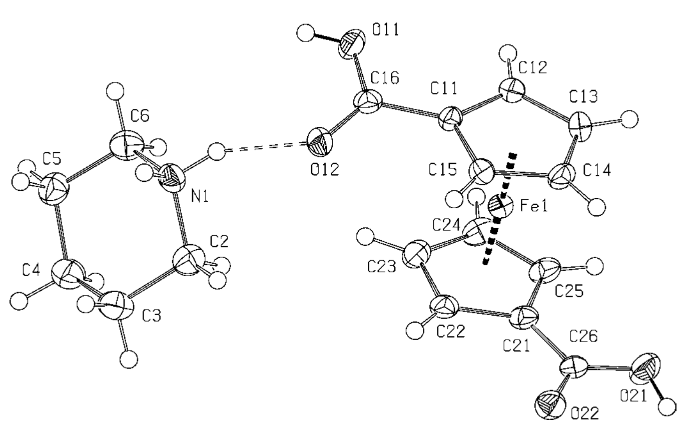

Figure 13
The molecular components of (6), showing the atom-labelling scheme: the H-atom sites adjacent to O11 and O21 have 0.50 occupancy. Displacement ellipsoids are drawn at the 30% probability level.

Subject to this disorder, O11 and O21 in the ferrocene unit at (x, y, z) form hydrogen bonds with O21 and O11 in the units at ($1 - x$, $-\frac{1}{2} + y$, $\frac{1}{2} - z$) and ($1 - x$, $\frac{1}{2} + y$, $\frac{1}{2} - z$), respectively, so producing a $C(8)$ chain running parallel to the [010] direction and generated by the 2_1 screw axis along ($\frac{1}{2}$, y, $\frac{1}{4}$) (Fig. 14). Two such chains, related by the centres of inversion, run through each unit cell. These chains are linked into sheets by the cations: N1 at (x, y, z) acts as hydrogen-bond donor *via* H1A to O12, also at (x, y, z), a component of the $C(8)$ chain along ($\frac{1}{2}$, y, $\frac{1}{4}$). The same N1 also forms, *via* H1B, a three-centre hydrogen bond (Table 2) in which the two acceptors are O11 at ($1 + x$, y, z) and O22 at ($2 - x$, $-\frac{1}{2} + y$, $\frac{1}{2} - z$), both of which are components of the $C(8)$ chain along ($\frac{3}{2}$, y, $\frac{1}{4}$). Similarly, N1 at ($1 - x$, $\frac{1}{2} + y$, $\frac{1}{2} - z$) is hydrogen-bond donor to O12 at ($1 - x$, $\frac{1}{2} + y$, $\frac{1}{2} - z$), a component of the chain along ($\frac{1}{2}$, y, $\frac{1}{4}$), and also to O11 at ($-x$, $\frac{1}{2} + y$, $\frac{1}{2} - z$) and O22 at ($-1 + x$, y, z), both of which are components of the chain along ($-\frac{1}{2}$, y, $\frac{1}{4}$). In this manner, all of the [010] chains within the domain $-0.02 < z < 0.52$ are linked into a sheet parallel to (001). A second such sheet, related to the first by the centres of inversion, lies in the domain $0.48 < z < 1.02$. There are no hydrogen bonds between adjacent sheets, so the supramolecular aggregation is strictly two-dimensional; the only significant C—H···O hydrogen bond (Table 2) lies within a (001) sheet.

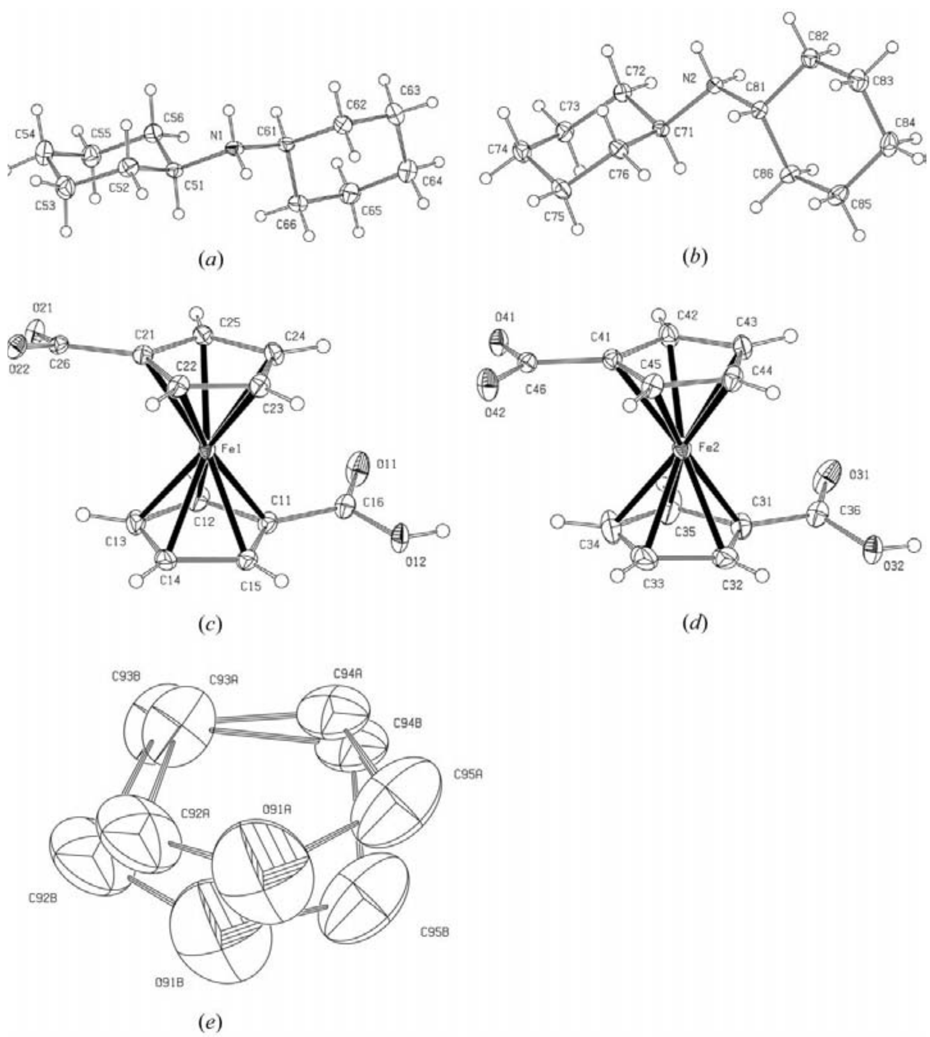

Figure 15
The five individual ionic components of (7), showing the atom-labelling scheme: (a) and (b) the two cations; (c) and (d) the two anions; and (e) the disordered solvent THF. Displacement ellipsoids are drawn at the 30% probability level.

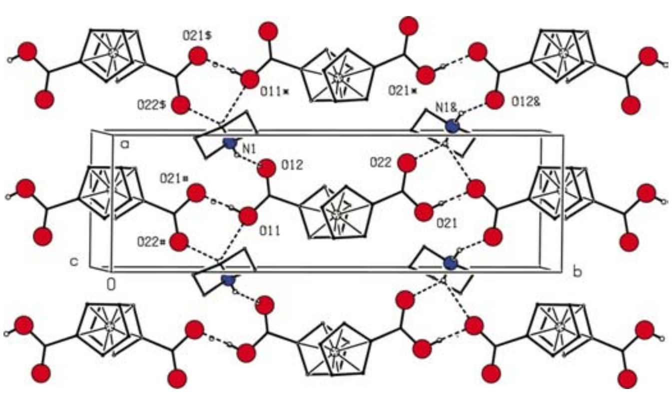

Figure 14
Part of the crystal structure of (6), showing the formation of a (001) sheet by the hard hydrogen bonds. For the sake of clarity, H atoms bonded to C are omitted. The atoms marked with a star (*), hash (#), dollar sign ($) or ampersand (&) are at the symmetry positions ($1 + x$, y, z), ($1 - x$, $-\frac{1}{2} + y$, $\frac{1}{2} - z$), ($2 - x$, $-\frac{1}{2} + y$, $\frac{1}{2} - z$) and ($2 - x$, $\frac{1}{2} + y$, $\frac{1}{2} - z$), respectively.

Di(cyclohexyl)ammonium(1+) ferrocene-1-carboxylic acid-1′-carboxylate(1−) tetrahydrofuran hemisolvate, (7). This salt crystallizes from tetrahydrofuran (C_4H_8O, THF) as a hemisolvate: $2[(C_6H_{11})_2NH_2^+].2[Fe(C_5H_4COO)(C_5H_4COOH)]^-.C_4H_8O$, where the asymmetric unit (Fig. 15) contains two independent di(cyclohexyl)ammonium cations and two independent ferrocenyl monoanions together with a molecule of THF in which all atoms are disordered over two sets of sites having equal occupancy. The cations and anions are linked into continuous sheets by six hard hydrogen bonds, four of N—H···O type and two of O—H···O type (Table 2). While there are also some soft C—H···O hydrogen bonds, these all lie within the sheets and hence do not influence the overall dimensionality of the supramolecular structure.

The formation of the sheet structure is readily analysed in terms of a one-dimensional substructure formed by the anions alone and thence of the linking of these anion chains by centrosymmetrically paired cations.

Within the asymmetric unit (Fig. 15), carboxyl O12 in the type 1 anion (containing Fe1) acts as hydrogen-bond donor to carboxylate O41 in the type 2 anion (containing Fe2); similarly, carboxyl O32 in the type 2 anion at (x, y, z) acts as donor to carboxylate O21 in the type 1 anion at ($1 + x$, y, z). In this way, a $C_2^2(16)$ chain is generated by translation along [100] (Fig. 16). In both of the O—H···O hydrogen bonds in this chain, the acceptor is one of the anionic carboxylate O atoms and the H···O and O···O distances are accordingly very short, with nearly linear O—H···O groups (Table 2). Two antiparallel anion chains, related by centres of inversion, run through each unit cell.

The anion chains are linked by pairs of cations. Within the asymmetric unit, N1 and N2 act as hydrogen-bond donors, *via* H1*A* and H2*A*, respectively, to the carboxylate atoms O41 and O21, respectively. Ammonium N1 at (x, y, z) also acts as donor, *via* H1*B*, to carboxylate O42 at ($1 - x$, $-y$, $-z$), while N1 at ($1 - x$, $-y$, $-z$) similarly acts as donor to O42 at (x, y, z), so forming a centrosymmetric $R_4^4(12)$ ring, centred at ($\frac{1}{2}$, 0, 0), linking two antiparallel $C_2^2(16)$ chains (Fig. 16). Between $R_4^4(12)$ rings centred at ($n + \frac{1}{2}$, 0, 0) (n = zero or integer) there are $R_8^6(40)$ rings centred at (n, 0, 0) (n = zero or integer). In an entirely similar way, N2 at (x, y, z) acts as hydrogen-bond donor, *via* H2*B*, to O22 at ($-1 - x$, $1 - y$, $1 - z$) and propagation of this interaction generates an independent series of $R_4^4(12)$ rings centred at ($n + \frac{1}{2}$, $\frac{1}{2}$, $\frac{1}{2}$) (n = zero or integer) separated by a further series of $R_8^6(40)$ rings centred at ($n, \frac{1}{2}, \frac{1}{2}$) ($n$ = zero or integer) (Fig. 16). The overall supramolecular structure thus consists of neutral sheets running parallel to ($01\bar{1}$), with just one sheet running through each unit cell.

The sheets occupy only *ca* 88% of the unit-cell volume, leaving two voids related by the centres of inversion in which the THF molecules are located. There are no hydrogen bonds or other directed intermolecular interactions involving the solvent molecules, which possibly contributes to their positional disorder.

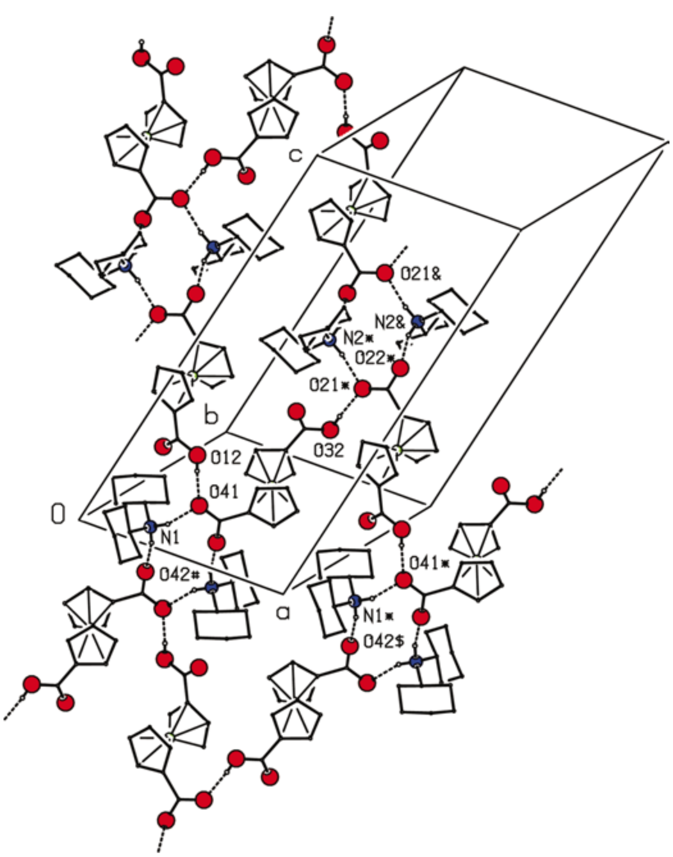

Figure 16
Part of the crystal structure of (7), showing the formation of a ($01\bar{1}$) sheet by the hard hydrogen bonds. For the sake of clarity, H atoms bonded to C are omitted. The atoms marked with a star (*), hash (#), dollar sign ($) or ampersand (&) are at the symmetry positions ($1 + x$, y, z), ($1 - x$, $-y$, $-z$), ($2 - x$, $-y$, $-z$) and ($-x$, $1 - y$, $1 - z$), respectively.

3.3. Hard hydrogen bonds produce three-dimensional structures

3.3.1. Bis[tri(ammonioethyl)amine(3+)] tris[ferrocene-1,1′-dicarboxylate(2−)], (8). The adduct (8) formed between

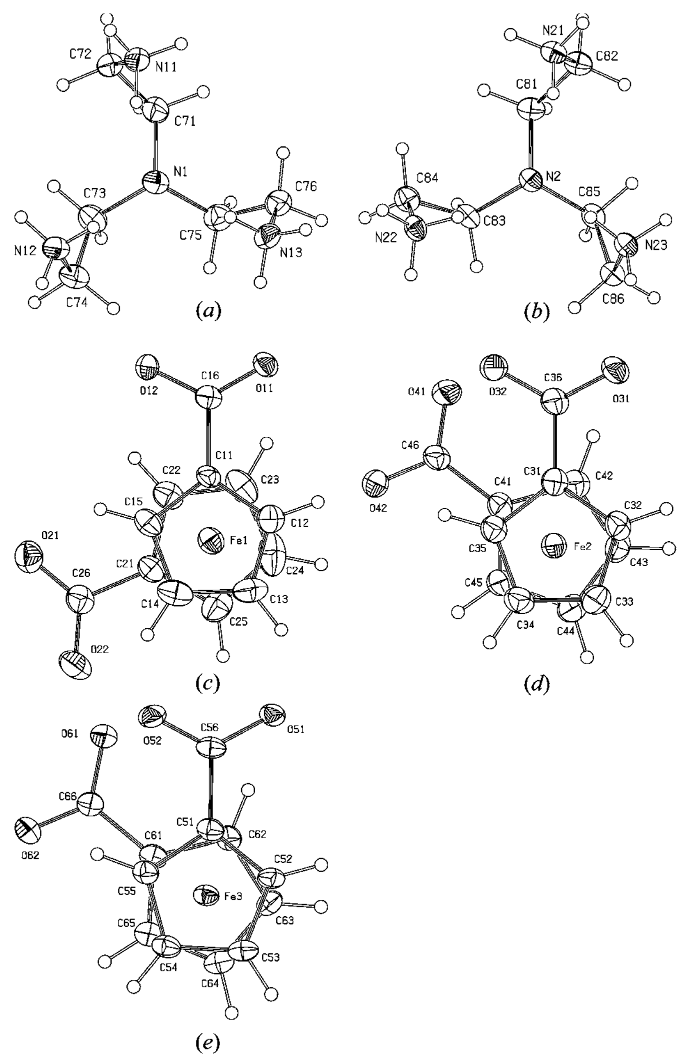

Figure 17
The five individual ionic components of (8), showing the atom-labelling scheme: (*a*) and (*b*), the two cations; (*c*)–(*e*), the three anions. Displacement ellipsoids are drawn at the 30% probability level.

tris(2-aminoethyl)amine and ferrocene-1,1′-dicarboxylic acid is a salt $2[N(CH_2CH_2NH_3)_3^{3+}].3[Fe(C_5H_4COO)]^{2-}$, characterized by complete transfer of H from O to N, so that all the H-atom sites are fully ordered. There are five independent ions in the asymmetric unit (Fig. 17), and each of the cations acts as a ninefold donor in N—H···O hydrogen bonds; while the anion of type 1 (containing Fe1) accepts four N—H···O hydrogen bonds, the other two anions (types 2 and 3, containing Fe2 and Fe3, respectively) both act as sevenfold acceptors. The number of N—H···O hydrogen bonds accepted by individual O atoms ranges from zero (O11) to three (O42 and O51).

The 18 independent N—H···O hydrogen bonds in the structure link the five independent ions into a single three-dimensional framework. As usual in such circumstances, the specification of the asymmetric unit permits considerable discretion but, in this case, it is possible to select a rather compact asymmetric unit such that ten of the 18 hard hydrogen bonds occur within the asymmetric unit (Fig. 18). It is then straightforward to identify supramolecular motifs that run in the [100], [010] and [001] directions, linking these five-component aggregates into a single whole.

Within the selected asymmetric unit, N13 acts as hydrogen-bond donor, *via* H13*A*–H13*C*, respectively, to O42, O62 and O22 (Table 2), so that cation 1 (containing N1) is directly linked to all three anions. In addition, both N11 and N12 act as donors, *via* H11*A* and H12*A*, respectively, to O42, and N12 acts as donor to O32, *via* H12*B*. The type 2 cation (containing N2) is directly linked to only two of the anions, in each case *via* paired N—H···O hydrogen bonds involving both carboxylate groups. Atoms N21 and N22 are donors, *via* H21*A* and H22*B*, respectively, to O21 and O12, respectively, in the type 1 anion, while N21 and N23 are donors, *via* H21*B* and H23*A*, to O61 and O52 in the type 3 anion. The two $R_2^2(16)$ motifs thus formed are mirrored by a third such motif involving cation 1 and anion 2.

The three-dimensional framework linking the five-component aggregates can be conveniently, although arbitrarily, defined in terms of three chain motifs, of steadily increasing complexity, running parallel to the principal axial directions. The chain parallel to [100] contains just two of the five ions: in cation 1, N11 at (x, y, z) acts as hydrogen-bond donor *via* H11*A* and H11*C*, respectively, to O42 in the type 2 anion, also at (x, y, z), and to O31 in the type 2 anion at $(1 + x, y, z)$. There is thus a $C_2^2(10)$ chain running parallel to the [100] direction, generated by translation and involving only one cation and one anion (Fig. 19). The motif parallel to [010] involves two cations and two anions: N13 in cation 1 at (x, y, z) acts as hydrogen-bond donor, *via* H13*C* and H13*B*, respectively, to O22 and O62 in the anions of type 1 and 3, both at (x, y, z). In the same three-component aggregate at (x, y, z), O12 acts as hydrogen-bond acceptor from N22 in the type 2 cation at $(1 - x, 2 - y, -z)$ and O51 acts as acceptor from N22 at $(1 - x, 1 - y, -z)$. Thus these four ions generate a $C_4^4(20)$ chain parallel to the [010] direction (Fig. 20).

The [001] chain motif is somewhat more complex than the [100] and [010] chains. In the anion of type 3 at (x, y, z), O61 and O62 accept hydrogen bonds from N21 and N13, both also at (x, y, z). In similar fashion, N13 in cation 1 at $(1 - x, 1 - y, -z)$ acts as donor, *via* H13*A* and H13*B*, respectively, to O42 and O62, both also at $(1 - x, 1 - y, -z)$. These two three-component aggregates are linked by further hydrogen bonds to form the [100] chain: N21 at (x, y, z) acts as donor, *via* H21*C*, to O51 at $(1 - x, 1 - y, -z)$, and N11 and N12 at (x, y, z) act as donors, *via* H11*B* and H12*C*, to O32 and O41, respectively, both at $(1 - x, 1 - y, 1 - z)$. In this manner, the two cations and two of the anions (types 2 and 3) combine to generate a $C_6^6(28)C_6^6(32)[R_2^2(16)]$ chain of rings parallel to [001] (Fig. 21).

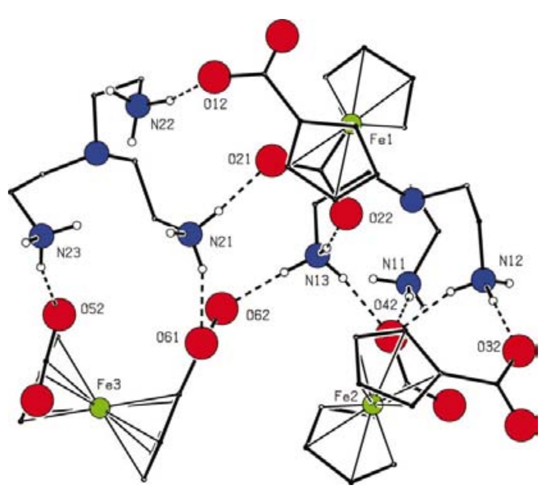

Figure 18
The asymmetric unit of (8), in which the five ionic components are linked by ten hydrogen bonds. For the sake of clarity, H atoms bonded to C are omitted.

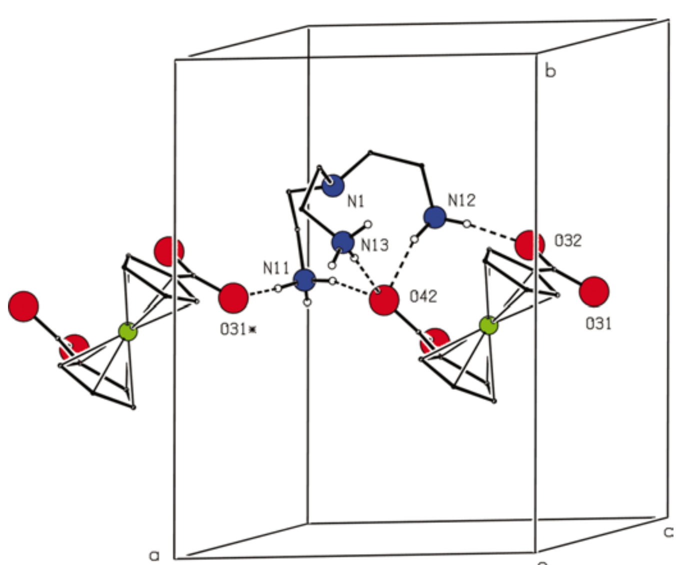

Figure 19
Part of the crystal structure of (8), showing the formation of a [100] chain. For the sake of clarity, H atoms bonded to C are omitted. The atom marked with a star (*) is at the symmetry position $(1 + x, y, z)$.

3.3.2. Bis[2-(4-hydroxyphenyl)ethylammonium(1+)] ferrocene-1,1′-dicarboxylate(2−), (9). This compound is a salt, $2(HOC_6H_4CH_2CH_2NH_3^+).[Fe(C_5H_4COO)_2]^{2-}$, crystallizing in space group $P\overline{1}$ with $Z' = 1.5$ and five independent ionic components in the asymmetric unit. The anion of type 1, containing Fe1, lies across a centre of inversion, chosen for convenience as that at $(\frac{1}{2}, \frac{1}{2}, \frac{1}{2})$. The type 2 anion (containing Fe2) and the cations of types 1–3 (containing N4, N5 and N6, respectively) all lie in general positions (Fig. 22). All of the independent N—H and O—H bonds participate in the hydrogen bonding (Table 2), such that the ions are linked into a single three-dimensional framework by nine N—H···O and three O—H···O hydrogen bonds. Five of the six carboxylate O atoms act as double acceptors of hydrogen bonds; one carboxylate O (O22) and O5 in the type 2 cation act as single acceptors.

It is possible to specify a fairly compact asymmetric unit (Fig. 23) such that the two anions and the cations of types 1 and 2 form an $R_4^4(30)$ ring from which the type 3 cation is pendent. The unit-cell contents thus comprise a centrosymmetric aggregate of nine ions, six cations and three anions. Five of the 12 independent hydrogen bonds lie within the asymmetric unit, leaving seven N—H···O hydrogen bonds available to generate the framework structure. The formation of this framework is most readily analysed in terms of the one-dimensional hydrogen-bond motifs that link the centrosymmetric nine-component aggregates. Four of the N—H···O hydrogen bonds generate motifs running parallel to the [100], [010] and [001] directions, and these are sufficient to generate the three-dimensional framework. The remaining three independent N—H···O hydrogen bonds generate further one-dimensional motifs running parallel to the [110], [101] and [111] directions, respectively, and it is convenient to consider each motif in turn.

Ions at the symmetry positions (x, y, z) and $(1 - x, 1 - y, 1 - z)$ lie in the nine-component aggregate centred at $(\frac{1}{2}, \frac{1}{2}, \frac{1}{2})$; within this, N5 at (x, y, z) acts as hydrogen-bond donor, *via* H5*A* and H5*C*, to carboxylate O31 and phenolic O5, respec-

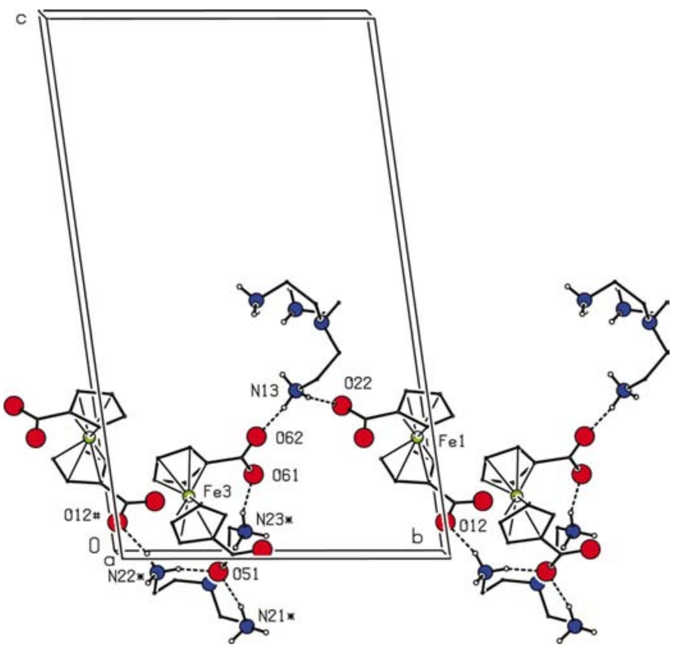

Figure 20
Part of the crystal structure of (8), showing the formation of a [010] chain. For the sake of clarity, H atoms bonded to C are omitted. The atoms marked with a star (*) or hash (#) are at the symmetry positions $(1 - x, 1 - y, -z)$ and $(x, -1 + y, z)$, respectively.

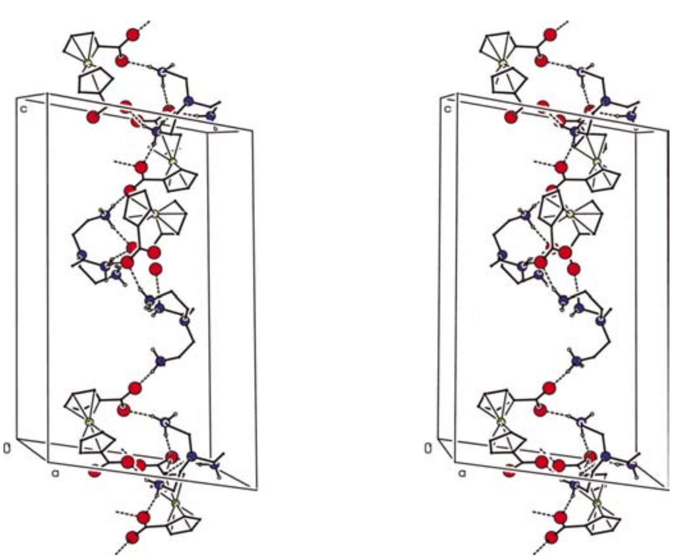

Figure 21
Stereoview of part of the structure of (8), showing the formation of a [001] chain.

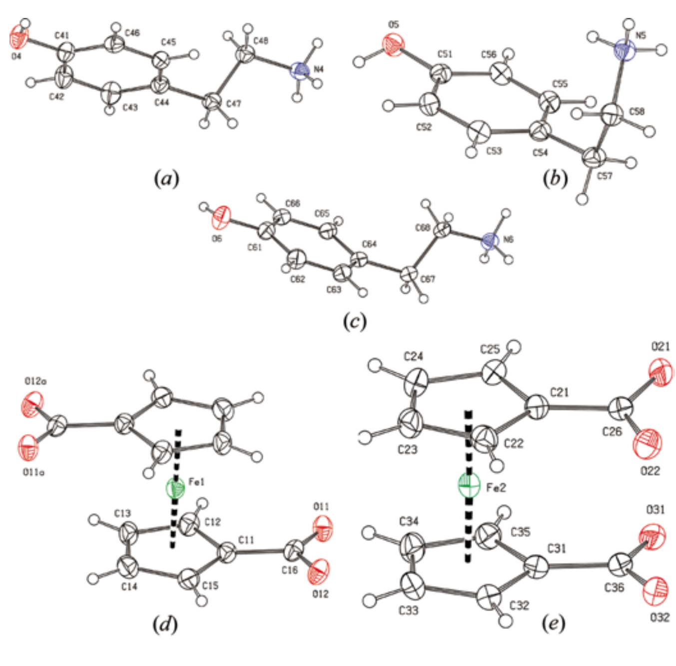

Figure 22
The five individual ionic components of (9), showing the atom-labelling scheme: (*a*)–(*c*) the three cations; (*d*) and (*e*) the two anions. Displacement ellipsoids are drawn at the 30% probability level. In (*d*), the atoms marked 'a' are at the symmetry position $(1 - x, 1 - y, 1 - z)$.

tively, both at $(-x, 1-y, 1-z)$ and thus both forming part of the aggregate centred at $(-\frac{1}{2}, \frac{1}{2}, \frac{1}{2})$. A $C_3^3(19)C_4^4(27)[R_3^3(12)]$ chain of rings running parallel to [100] is thus produced (Fig. 24). Similarly, N6 at (x, y, z) acts as hydrogen-bond donor, *via* H6*C*, to carboxylate O21 at $(x, -1+y, z)$, so generating a $C_2^2(17)$ chain running parallel to [010] (Fig. 25). Within the nine-component aggregate centred at $(\frac{1}{2}, \frac{1}{2}, \frac{1}{2})$, N4 at (x, y, z) acts as hydrogen-bond donor, *via* H4*B*, to carboxylate O12 at $(1-x, 1-y, -z)$, which is part of the aggregate centred at $(\frac{1}{2}, \frac{1}{2}, -\frac{1}{2})$: in this way a $C_2^2(17)$ chain running parallel to [001] is produced (Fig. 26). The combination of the three simple one-dimensional motifs is sufficient to generate the three-dimensional framework, but these motifs do not utilize all of the hydrogen bonds

The three remaining N—H···O hydrogen bonds, involving only N4 and N6 as donors and O11 and O32 as acceptors, generate three further one-dimensional motifs. N6 at (x, y, z) acts as hydrogen-bond donor, *via* H6*B*, to carboxylate O11 at $(-1+x, -1+y, z)$, so generating by translation a $C_4^3(28)$ chain running parallel to the [110] direction (Fig. 27). N4 at (x, y, z) acts as donor, *via* H4*C*, to carboxylate O32 at $(-x, 1-y, -z)$, part of the nine-component aggregate centred at $(-\frac{1}{2}, \frac{1}{2}, -\frac{1}{2})$, so producing a $C_4^4(34)$ chain running parallel to the [101] direction (Fig. 28). Finally, N6 at (x, y, z) acts as donor, *via* H6*A*, to O32 at $(-x, -y, -z)$, a component of the aggregate centred at $(-\frac{1}{2}, -\frac{1}{2}, -\frac{1}{2})$: in this manner, a $C_6^6(51)$ chain running parallel to the [111] direction is produced (Fig. 29).

3.4. Molecular conformations and dimensions

3.4.1. Ferrocene components. A convenient measure of the relative twist of the rings in 1,1′-disubstituted ferrocenes is the torsion angle C11—*Cg*(1)—*Cg*(2)—C21, where *Cg*(1) and *Cg*(2) are the centroids of the two rings: to allow for the fact that the rings do not have local C_5 rotational symmetry, because of the variations in the C—C bond distances, the mean value of the torsion angles C*pn*—*Cg*(*p*)—*Cg*(*q*)—C*qn*

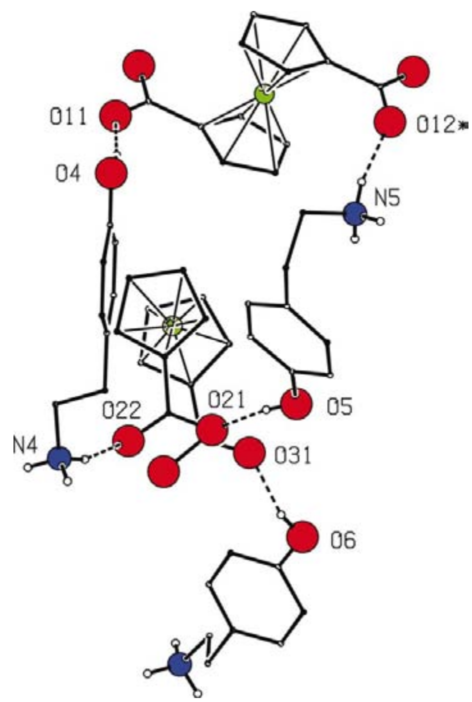

Figure 23
The asymmetric unit of (9), in which the five ionic components are linked by five hydrogen bonds. For the sake of clarity, H atoms bonded to C are omitted. The atom marked with a star (*) is at the symmetry position $(1-x, 1-y, 1-z)$.

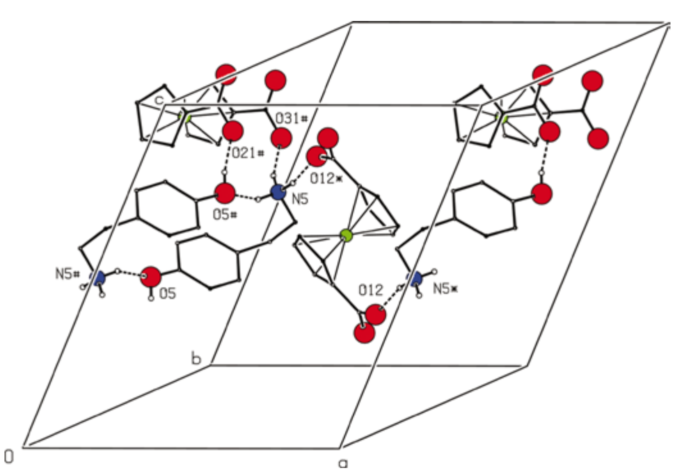

Figure 24
Part of the crystal structure of (9), showing the formation of a chain of rings along [100]. For the sake of clarity, H atoms bonded to C are omitted. The atoms marked with a star (*) or hash (#) are at the symmetry positions $(1-x, 1-y, 1-z)$ and $(-x, 1-y, 1-z)$, respectively.

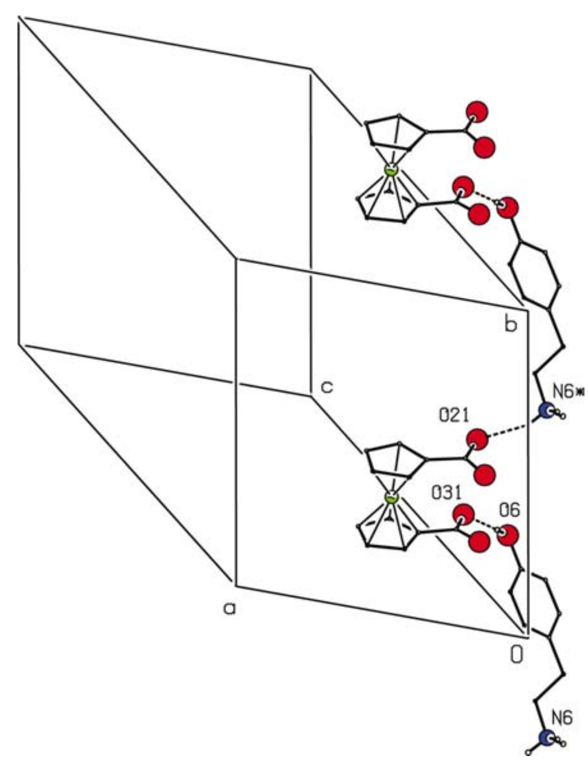

Figure 25
Part of the crystal structure of (9), showing the formation of a $C_2^2(17)$ chain parallel to [010]. For the sake of clarity, H atoms bonded to C are omitted. The atoms marked with a star (*) are at the symmetry position $(x, 1+y, z)$.

(where p, q define the cyclopentadienyl ring concerned and $n = 1$–5 defines the C atoms within those rings) provides a better measure. If we define a parameter m as the integer approximation to the mean value of [Cpn—$Cg(p)$—$Cg(q)$—Cqn]/36, or alternatively the mean torsional angle is approximated by $m(\pi/5)$ radians, then the value of m provides a simple and convenient descriptor of the conformation. In particular, eclipsed conformations have even values of m (0, 2 or 4), while staggered conformers have odd values (1, 3 or 5).

Table 3 lists the mean values of the torsional angles Cpn—$Cg(p)$—$Cg(q)$—Cqn, together with the corresponding values of m, for (1)–(9). Of the staggered conformers, that having $m = 5$, representing exactly or approximately centrosymmetric ferrocene units, is present in (2), (4), (5) and (9), and the other staggered conformers, having $m = 1$ or 3, both occur in (8). The eclipsed conformers, with even values of m, occur in (1), (3), (6), (7) and (9). It is noteworthy that in (9) the two extreme conformers having $m = 0$ and 5, respectively, occur concurrently, whereas both independent anions in (7) have $m = 4$, and all of the anions in (8) have odd values of m. The observation within this series of compounds of the complete conformational spectrum testifies to the effectively free rotation of the rings relative to one another and indicates that the actual conformation observed in any system is probably dominated by the direction-specific intermolecular forces, primarily the hard hydrogen bonds

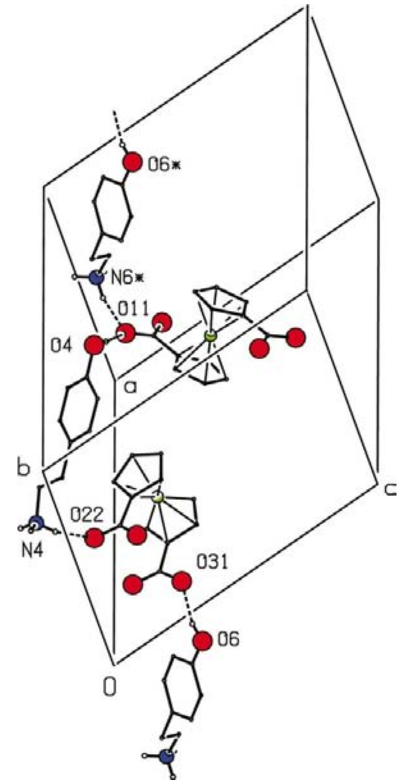

Figure 27
Part of the crystal structure of (9), showing the formation of a $C_4^3(28)$ chain along [110]. For the sake of clarity, H atoms bonded to C are omitted. The atoms marked with a star (*) are at the symmetry position $(1 + x, 1 + y, z)$.

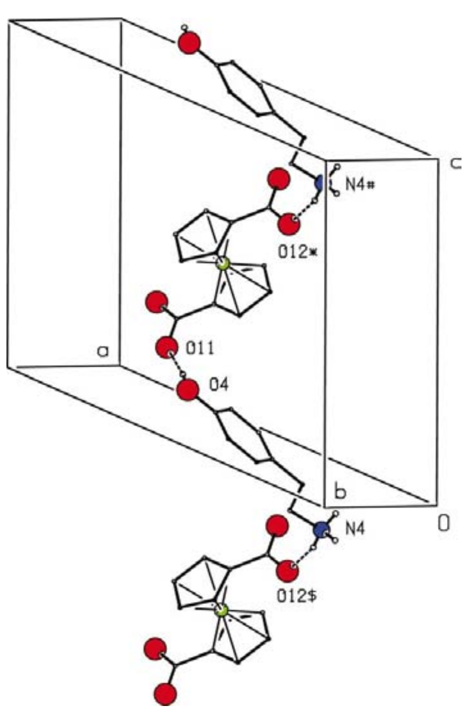

Figure 26
Part of the crystal structure of (9), showing the formation of a $C_2^2(17)$ chain parallel to [001]. For the sake of clarity, H atoms bonded to C are omitted. The atoms marked with a star (*), hash (#) or dollar sign ($) are at the symmetry positions $(1 - x, 1 - y, 1 - z)$, $(x, y, 1 + z)$ and $(1 - x, 1 - y, -z)$, respectively.

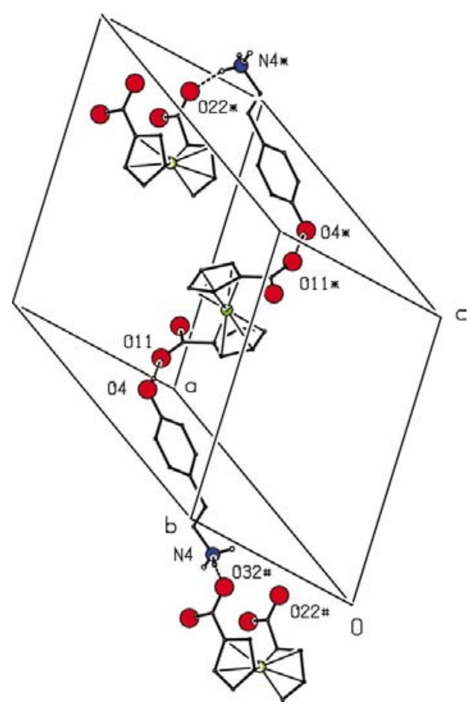

Figure 28
Part of the crystal structure of (9), showing the formation of a $C_4^4(34)$ chain along [101]. For the sake of clarity, H atoms bonded to C are omitted. The atoms marked with a star (*) or hash (#) are at the symmetry positions $(1 - x, 1 - y, 1 - z)$ and $(-x, 1 - y, -z)$, respectively.

Staggered conformers with $m = 3$ or 5 and eclipsed conformers with $m = 2$ occur in amidine adducts (Braga, Maini, Grepioni *et al.*, 2000), and conformers having $m = 3$, 4 and 5 occur in organometallic salts (Braga, Maini & Grepioni, 2000).

3.4.2. Amine components. The morpholine and piperidine components in (3) and (6), respectively, and all of the cyclohexyl rings in (7) adopt the usual chair conformation (Figs. 6, 13 and 15) and require no further comment.

The conformational properties of the DABCO molecule have been extensively investigated, both in the solid state (Weiss *et al.*, 1964; Nimmo & Lucas, 1976; Mak *et al.*, 1984) and in the gas phase (Yokozeki & Kuchitsu, 1971). The principal point of interest is the extent of any twist of the molecule from ideal D_{3h} symmetry by internal rotation about the N···N vector: in the D_{3h} conformation, the neighbouring CH_2 groups are all eclipsed. For isolated molecules in the gas phase (Yokozeki & Kuchitsu, 1971), the internal dynamics indicated a very broad potential well for the twist motion, best fitted by a harmonic quartic potential function having an energy minimum corresponding to a twist of *ca* 10° from the D_{3h} geometry. In (2), the N—C—C—N torsion angles range from 2.1 (3) to 3.4 (3)°, indicative of a small but real distortion of the DABCO skeleton from the fully eclipsed conformation.

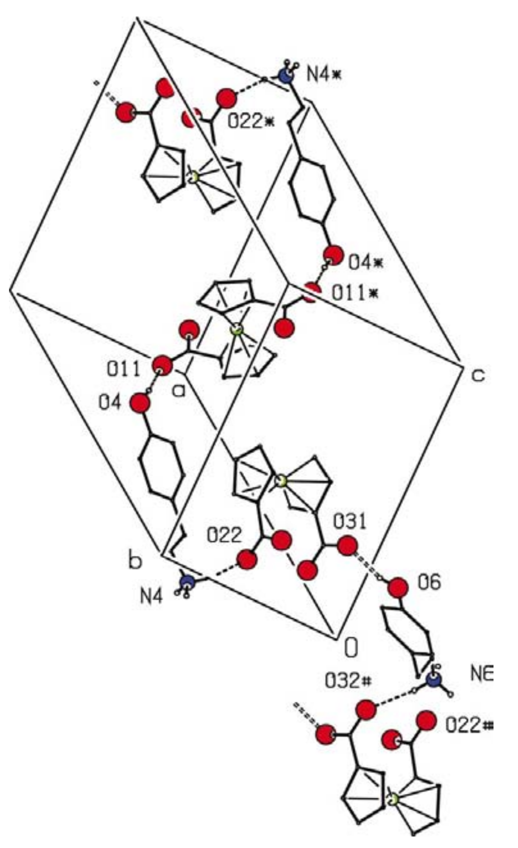

Figure 29
Part of the crystal structure of (9), showing the formation of a $C_6^6(51)$ chain along [111]. For the sake of clarity, H atoms bonded to C are omitted. The atoms marked with a star (*) or hash (#) are at the symmetry positions $(1 - x, 1 - y, 1 - z)$ and $(-x, -y, -z)$, respectively.

Distortions of a similar magnitude have been observed in the 1:1 adduct of hydroquinone with DABCO (Mak *et al.*, 1984) and in the 2:1 adducts of phenol with DABCO (Mak *et al.*, 1984) and of phenylphosphonic acid with DABCO (Ferguson *et al.*, 1998).

Although the 4,4′-bipyridyl unit in (4) could readily lie across a centre of inversion, in fact it lies in a general position in space group $P\bar{1}$, with a considerable twist away (Table 4) from the idealized conformation having parallel rings. The N—C—C—C and C—C—C—C torsional angles in the amine components of (5) are all within 3° of 180°, indicative of a completely staggered all-*trans* extended chain conformation. The two independent cations in (8) both adopt conformations that are very close to $C3$ molecular symmetry (Table 4); thus each cation is chiral and the two cations in the selected asymmetric unit are effectively enantiomeric (Fig. 17). However, the pattern of the hydrogen bonds formed by these cations (Table 2) unambiguously rules out any possibility of additional crystallographic symmetry.

Two of the independent cations in (9), those containing N4 and N6, adopt conformations that are effectively enantiomeric (Table 4, Fig. 22), but again their hydrogen-bonding characteristics are entirely different (Table 2). This observation is of some importance in ruling out any possibility of additional symmetry, as a Z' value of 1.5 is highly unusual in space group $P\bar{1}$ (Brock & Dunitz, 1994). On the other hand, the conformation of the cation containing N5 differs markedly from those of the other two cations (Table 4).

4. Conclusion

In (1)–(9), the supramolecular aggregation is dominated by hard hydrogen bonds of O—H···O, O—H···N and N—H···O types, although in several examples there are soft C—H···O hydrogen bonds that are structurally significant and in (2)–(4) these soft hydrogen bonds expand the dimensionality of the overall structure. Since in the majority of compounds the individual components are ionic, the hard hydrogen bonds in general have H···A and D···A distances that are short for their types, as expected for charge-assisted hydrogen bonds. However, we also note that amongst the soft hydrogen bonds the shortest H···A and D···A distances, as well as the largest D—H···A angles, are observed in (4), in which, uniquely within this series, both components are overall neutral, with no H transfer from O to N having occurred. The intrinsic polarity of the heteroaromatic C—H bonds apparently has an importance here comparable to that of charge assistance in aliphatic systems.

X-ray data were collected at the University of Toronto using a Nonius KappaCCD diffractometer purchased with funds from NSERC (Canada). CMZ thanks the Association of Commonwealth Universities for the award of a Commonwealth Fellowship 2000–2001.

References

Braga, D., Grepioni, F., Biradha, K., Pedireddi, V. R. & Desiraju, G. R. (1995). *J. Am. Chem. Soc.* **117**, 3156–3166.

Braga, D., Maini, L. & Grepioni, F. (2000). *J. Organomet. Chem.* **593**, 101–108.

Braga, D., Maini, L., Grepioni, F., de Cian, A., Félix, O., Fischer, J. & Hoseini, M. W. (2000). *New J. Chem.* **24**, 547–553.

Brock, C. P. & Dunitz, J. D. (1994). *Chem. Mater.* **6**, 1118–1127.

Ferguson, G. (1999). *PRPKAPPA*. University of Guelph, Canada.

Ferguson, G., Gallagher, J. F., Glidewell, C. & Zakaria, C. M. (1993). *J. Chem. Soc. Dalton Trans.* pp. 3499–3506.

Ferguson, G., Glidewell, C., Gregson, R. M. & Meehan, P. R. (1998). *Acta Cryst.* B**54**, 129–138.

Ferguson, G., Glidewell, C., Lewis, A. & Zakaria, C. M. (1995). *J. Organomet. Chem.* **492**, 229–234.

Glidewell, C., Ferguson, G., Lough, A. J. & Zakaria, C. M. (1994). *J. Chem. Soc. Dalton Trans.* pp. 1971–1982.

Mak, T. C. W., Yip, W.-H. & Book, L. (1984). *J. Crystallogr. Spectrosc. Res.* **14**, 457–465.

Nimmo, J. K. & Lucas, B. W. (1976). *Acta Cryst.* B**32**, 348–353.

Nonius B. V. (1997). *KappaCCD Server Software.* Windows 3.11 Version. Delft, The Netherlands.

Otwinowski, Z. & Minor, W. (1997). *Methods Enzymol.* **276**, 307–326.

Palenik, G. J. (1969). *Inorg. Chem.* **8**, 2744–2749.

Sheldrick, G. M. (1997*a*). *SHELXL*97. University of Göttingen, Germany.

Sheldrick, G. M. (1997*b*). *SHELXS*97. University of Göttingen, Germany.

Spek, A. L. (2002). *PLATON*. Version of March 2002. University of Utrecht, The Netherlands.

Takusagawa, F. & Koetzle, T. F. (1979). *Acta Cryst.* B**35**, 2888–2896.

Weiss, G. S., Parkes, A. S., Nixon, E. R. & Hughes, R. E. (1964). *J. Chem. Phys.* **41**, 3759–3767.

Wilson, A. J. C. (1976). *Acta Cryst.* A**32**, 994–996.

Yokozeki, A. & Kuchitsu, K. (1971). *Bull. Chem. Soc. Jpn*, **44**, 72–77.

Zakaria, C. M., Ferguson, G., Lough, A. J. & Glidewell, C. (2001). *Acta Cryst.* C**57**, 914–917.

Zakaria, C. M., Ferguson, G., Lough, A. J. & Glidewell, C. (2002*a*). *Acta Cryst.* C**58**, m1–m4.

Zakaria, C. M., Ferguson, G., Lough, A. J. & Glidewell, C. (2002*b*). *Acta Cryst.* C**58**, m5–m7.